NASA TECHNICAL NOTE

NASA TN D-5983

NASA TN D-5983

FIXED-BASE VISUAL-SIMULATION STUDY OF MANUALLY CONTROLLED OPERATION OF A LUNAR FLYING VEHICLE

by G. Kimball Miller, Jr., and Gene W. Sparrow

Langley Research Center
Hampton, Va. 23365

NATIONAL AERONAUTICS AND SPACE ADMINISTRATION • WASHINGTON, D. C. • DECEMBER 1970

1. Report No.	2. Government Accession No.	3. Recipient's Catalog No.
NASA TN D-5983		

4. Title and Subtitle	5. Report Date
FIXED-BASE VISUAL-SIMULATION STUDY OF MANUALLY CONTROLLED OPERATION OF A LUNAR FLYING VEHICLE	December 1970
	6. Performing Organization Code
7. Author(s)	8. Performing Organization Report No.
G. Kimball Miller, Jr., and Gene W. Sparrow	L-7320
	10. Work Unit No.
9. Performing Organization Name and Address	127-51-34-03
NASA Langley Research Center Hampton, Va. 23365	11. Contract or Grant No.
	13. Type of Report and Period Covered
12. Sponsoring Agency Name and Address	Technical Note
National Aeronautics and Space Administration Washington, D.C. 20546	14. Sponsoring Agency Code

15. Supplementary Notes

16. Abstract

A fixed-base visual-simulation study has been conducted to determine the instrumentation and control requirements for operating a lunar flying vehicle over a range of about 2.25 nautical miles (4.167 km). The study indicated that a rate-command attitude control system was required for small center-of-gravity offsets. The average characteristic velocity required to fly a 500-foot-altitude (152.4-m) flat-top trajectory to the target was 1197.6 ft/sec (365.0 m/sec) with a standard deviation of 199.0 ft/sec (60.6 m/sec) when the instrumentation used included a three-axis gyro-horizon, a fuel indicator, a lunar thrust-weight-ratio indicator, and an altimeter. When horizontal- and vertical-velocity indicators were included, the average characteristic velocity was reduced by approximately 150 ft/sec (45.7 m/sec) and the standard deviation by 100 ft/sec (30.5 m/sec). It was extremely difficult to perform the maneuver without velocity indicators or an altimeter.

17. Key Words (Suggested by Author(s))	18. Distribution Statement
Visual simulation Lunar flying vehicle	Unclassified – Unlimited

19. Security Classif. (of this report)	20. Security Classif. (of this page)	21. No. of Pages	22. Price*
Unclassified	Unclassified	41	$3.00

*For sale by the National Technical Information Service, Springfield, Virginia 22151

FIXED-BASE VISUAL-SIMULATION STUDY OF MANUALLY CONTROLLED OPERATION OF A LUNAR FLYING VEHICLE

By G. Kimball Miller, Jr., and Gene W. Sparrow
Langley Research Center

SUMMARY

A fixed-base visual-simulation study has been conducted to determine, within the limits of the simulation, the instrumentation and control characteristics necessary for a pilot to operate a typical lunar flying vehicle over a range of 2.25 n. mi. (4.167 km). The investigation employed a closed-circuit television system in conjunction with a front-lighted lunar terrain model for image generation. All six rigid-body degrees of freedom of the vehicle were provided. The pilot controlled the vehicle by means of a throttleable propulsion system in conjunction with a six-jet attitude control system.

The results of the initial phase of the investigation indicated that: (1) a rate-command attitude control system was required to control effectively the vehicle with center-of-gravity offsets of about 0.0067 foot (0.002 meter), (2) the rate deadband of the attitude control system should be approximately 0.2^{o}/sec, and (3) the main engine throttle sensitivity should be about $0.04g_m$ (lunar gravity) per degree of throttle deflection. During preliminary low-altitude flights using these characteristics, the pilots generally landed within approximately 150 feet (45.7 meters) of a selected landing site with touchdown velocities of less than 8 ft/sec (2.4 m/sec) vertically and 6 ft/sec (1.8 m/sec) horizontally.

The efficiency with which the pilots were able to perform long-range high-altitude flat-top trajectories to a selected landing site varied with the vehicle instrumentation. By using a three-axis gyro-horizon, a lunar thrust-weight-ratio indicator, a fuel indicator, and an altimeter, the simulated flights required an average characteristic velocity of 1197.6 ft/sec (365.0 m/sec) with a standard deviation of 199.0 ft/sec (60.6 m/sec). When horizontal- and vertical-velocity indicators were included, the average characteristic velocity was reduced by approximately 150 ft/sec (45.7 m/sec) and the standard deviation by about 100 ft/sec (30.5 m/sec). Flights performed without either an altimeter or velocity indicators required approximately the same characteristic velocity as the flights which used an altimeter. It should be emphasized, however, that only an extremely well trained pilot, familiar with the nominal flight profile, could adequately perform the

maneuver without an altimeter. The translational velocity used on a given flight varied considerably with the instrumentation employed. However, the dominant factor affecting fuel use was the time spent at near-hover conditions during descent to the landing site. Although the vehicle was capable of a lunar thrust-weight ratio of 3.0 with the vehicle fully loaded, the pilots never exceeded a value of about 1.8.

INTRODUCTION

There is currently considerable interest in devices for extending the range capabilities of lunar explorers for future lunar missions. Lunar flying vehicles are of primary concern because they permit explorations of many lunar features of scientific interest which are inaccessible by surface travel. In addition, extra-vehicular activity time at a remote site can be maximized. The Langley Research Center has initiated a research program in which full-scale manned lunar flying vehicles of various design configurations are to be flight tested by use of the lunar landing research facility. (See ref. 1.) Emphasis in this program is placed on studying vehicle handling qualities and is limited to low-altitude short-range maneuvers.

The present fixed-base simulation study includes a preliminary examination of handling-quality requirements. However, the present study was primarily conducted to determine, within the limits of the simulation, the instrumentation and control requirements for high-altitude long-range operation of a typical lunar flying vehicle. The general class of vehicle under consideration typically involves operation at altitudes on the order of 500 ft (152.4 meters) over a range of about 2.25 n. mi. (4.167 km). (See ref. 2.) The basic instrumentation used in the investigation consisted of a fuel indicator, a lunar thrust-weight ratio indicator, a three-axis gyro-horizon, and an altimeter. Selected flights employed vertical- and horizontal-velocity indicators. The pilot's view of the lunar surface was presented through a virtual image display. Scene generation was accomplished by using a closed-circuit television system and a front-lighted lunar terrain model. The equations of motion permitted six rigid-body degrees of freedom and were solved on a digital computer operating in real time.

EQUATIONS OF MOTION

The symbols used in the six-degree-of-freedom equations of motion employed in the present investigation are presented in appendix A. The formulation of these equations and the transformation matrices for the assumed axis systems are presented in appendix B. The form of the equations of motion and the axis systems used were dictated by the requirements of the simulation equipment. The force equations were written with respect to cylindrical coordinates, and the moment equations were written with respect to

body axes. The fixed-reference frame was located at the center of the moon which was assumed to be a nonrotating homogeneous sphere. The vehicle mass and moments of inertia were varied to account for mass reduction during main engine and reaction-control-system thrusting. The pilot closed the control loop through the use of a three-axis hand controller and a throttle.

VEHICLE DESCRIPTION

The simulated lunar flying vehicle had an empty lunar weight of approximately 43 pounds (191.3 newtons), a take-off weight of approximately 200 lunar pounds (889.6 newtons) (including astronaut and payload), and a characteristic velocity capability of about 4000 ft/sec (1219.2 m/sec). The propulsion system was throttleable from a lunar thrust-weight ratio T/W_o of 0.3 to 1.8 (sketch (a)) and was capable of a T/W_o of 3.0 for emergencies.

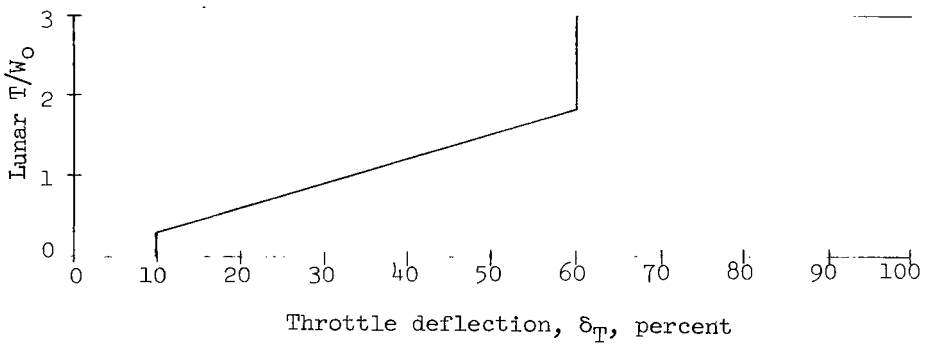

Sketch (a)

Vehicle attitude control was accomplished through the use of a three-axis hand controller which activated six on-off reaction control jets through a rate-command system capable of maximum rates of 20^o/sec about all axes. (Some flights were performed with an acceleration-command system which employed six reaction control jets with thrust levels that were proportional to controller deflection.) Center-of-gravity displacements from the vehicle thrust axis of ±0.0067 foot (±0.0020 meter) along the X and Y body axes were simulated. The center-of-gravity displacement along the thrust axis and the vehicle moments of inertia are presented in figure 1 as functions of the instantaneous vehicle mass.

The field of view from a typical lunar flying vehicle may be virtually unrestricted. However, the simulation equipment used in this investigation was capable of a visual cone of only 90^o. The simulated vehicle is depicted in sketch (b).

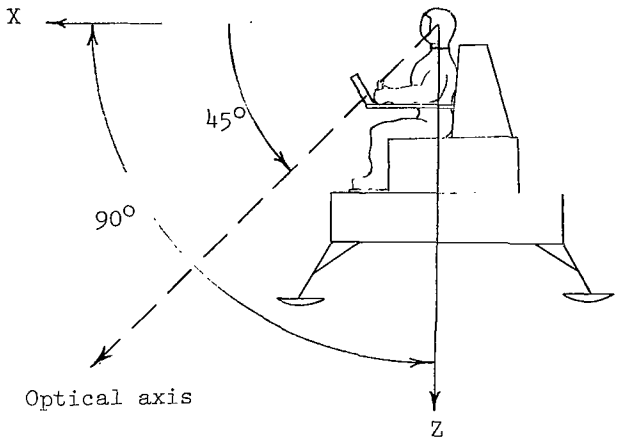

Sketch (b)

The simulated field of view in the pitch plane was approximately 90° about an optical axis that was angularly offset from the vehicle X-axis by 45°. The field of view in the XY-plane was approximately 90°. Thus, the pilots field of view, although limited, encompassed both the forward lunar horizon and the terrain directly beneath the simulated vehicle when the vehicle was in a vertical attitude.

SIMULATION EQUIPMENT

The simulation equipment used in the study is depicted in figure 2. The pilot's view of the lunar landscape was generated by a closed-circuit television system and a 16- by 20-foot (4.9- by 6.1-meter) lunar-terrain model that was scaled at 1200:1. (In addition, a 144:1 scale terrain model was used during a preliminary investigation.) The terrain model was frontlighted at a simulated sun angle of approximately 10°. (See fig. 3). An optical pickup, similar to that described in reference 3, was used in conjunction with an image orthicon television camera with 875 scan lines to obtain the three rotational degrees of freedom of the vehicle. The three translational degrees of freedom were obtained by mounting the optical pickup and camera combination on a transport system that moved relative to the terrain model in response to the output of the force equations. It should be noted that model protection considerations imposed a minimum altitude limit above the desired landing site of approximately 150 feet (45.7 meters), at which point an electrical stop was activated.

The visual scene was projected through a virtual-image-display system to enhance the simulation of depth, perspective, and spatial orientation. A mirror was mounted on the face of the virtual-image display to force a pilot seated in the fixed-base instrumented cockpit (fig. 4) to bend forward and look down in order to see the terrain beneath the

simulated lunar flying vehicle. The basic instrumentation was an altimeter with a resolution of 100 feet (30.5 meters); a fuel indicator with a resolution of 2 percent; a lunar thrust-weight ratio indicator with a resolution of 0.04; and a three-axis gyro-horizon. Additional instrumentation used at various times during the investigation were vertical- and horizontal-velocity indicators with resolution of 1 ft/sec (0.30 m/sec) and 5 ft/sec (1.52 m/sec), respectively. Vehicle thrust level was commanded through the use of a throttle located at the left of the pilot's seat. The throttle was a fingertip controller which moved fore and aft and required approximately 1 pound (4.45 newtons) of force to operate. It consisted of a lever 0.583 foot (0.178 meter) long which was pivoted at one end and had an angular throw of about 49°. Attitude control was provided through a rate-command system (occasionally acceleration command) by using a three-axis hand controller located to the right of the pilot's seat. The control-handle displacements were $\pm 15^{\circ}$ in pitch and $\pm 30^{\circ}$ in roll and yaw. The controller required 0.25 in-lb/deg (0.028 m-N/deg) outside deadbands of $\pm 1.5^{\circ}$ in pitch and $\pm 3.0^{\circ}$ in roll and yaw, with breakout torques of approximately 5 in-lb (0.56 m-N) for all axes.

TASK DESCRIPTION

The trajectory the pilots were asked to employ is typical (ref. 2) of those being considered for lunar flying vehicles and is depicted in sketch (c):

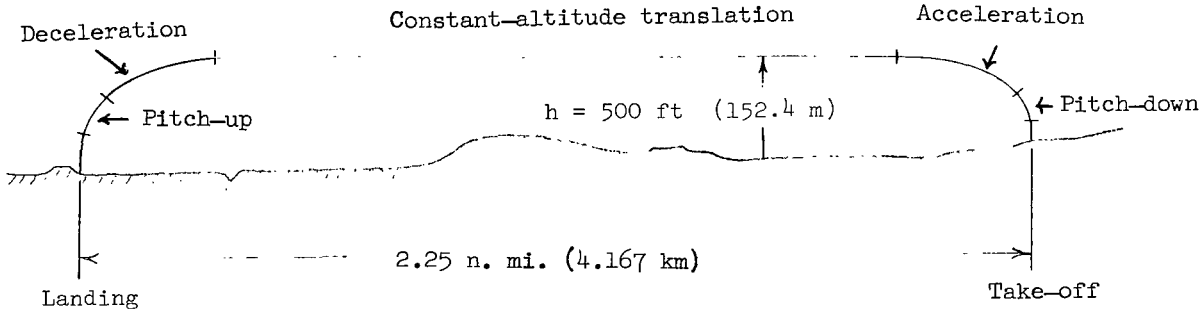

Sketch (c)

The pilot's task was to execute a 500-foot altitude (152.4-meter) flat-top trajectory to a landing site located approximately 2.25 n. mi. (4.167 km) from the take-off point. It was assumed that the pilot knew the approximate range and direction to the desired landing site prior to take-off and thus used a predetermined procedure. The simulated flights were initiated at an altitude of about 55 feet (16.8 meters) with the vehicle ascending vertically at 22 ft/sec (6.7 m/sec); this ascent corresponds to a 5-second vertical ascent at a lunar T/W of 1.8. The pilots were instructed to reduce T/W initially to 1.0 and to pitch the vehicle down about 9°/sec until a pitch angle of -45° was

attained, at which time the vehicle will have reached an altitude of approximately 500 feet (152.4 meters) and nearly zero vertical velocity. The pilots were then to increase T/W to 1.4 and accelerate the vehicle until they attained a cruise velocity that they felt was desirable. (The near-optimum cruise velocity of 200 ft/sec (61.0 m/sec) for this trajectory (ref. 2) requires approximately 31 seconds of acceleration.) The pilots then reduced T/W to 1.0 and pitched the vehicle up at about 9°/sec until the vehicle was vertical. The vehicle then translated at nearly constant altitude to a point near the desired landing site (approximately 32 seconds for the 200-ft/sec (61.0-m/sec) cruise velocity). The pilots then decelerated the vehicle by reversing the procedure used during the acceleration phase. After the deceleration phase, the pilot's task was to manipulate vehicle attitude and T/W to bring the vehicle horizontal velocity to nearly zero above the desired landing site and to descend vertically to the lunar surface. The landing site chosen for the simulation was defined by a 340-foot diameter (103.6-meter) crater located 2.25 n. mi. (4.167 km) downrange from the take-off point. The pilots were instructed to land outside the crater but as close to the crater rim as possible. Because of the 150-foot (45.7-meter) minimum altitude restriction existing in the simulation equipment, the pilot was instructed to bring the horizontal-velocity components to zero at an altitude slightly exceeding 150 feet (45.7 meters) and descend vertically toward the surface with descent rates less than 20 ft/sec (6.1 m/sec).

RESULTS AND DISCUSSION

Two research pilots and two research engineers acted as pilots during the present study, which was conducted in two phases. The first phase involved low-altitude short-range flights and was primarily concerned with the vehicle handling qualities. The second phase involved long-range flights with an emphasis on instrumentation requirements.

Low-Altitude Flights

A preliminary investigation using a terrain model scaled at 144:1 was conducted for two reasons: (1) to vary the vehicle control characteristics to obtain handling qualities that the research pilots felt were satisfactory and (2) to examine the pilots' performance from an altitude of 150 feet (45.7 meters) to touchdown (zero altitude could be simulated by using 144:1 scaling). During this phase of the investigation the pilot's task was to take off from a simulated lunar surface, climb to an altitude of approximately 150 feet (45.7 meters), translate about 450 feet (137.2 meters) to a target crater with a diameter of approximately 200 feet (61.0 meters), and land inside the crater rim with touchdown velocities of less than 10 ft/sec (3.05 m/sec) vertically and nearly zero horizontally.

Within the limits imposed by fixed-base simulation, the following determinations were made:

(1) Rate command attitude control is required for center-of-gravity offsets on the order of ±0.0067 foot (±0.002 meter). Center-of-gravity displacements of 0.0067 foot (0.002 meter) along the X and Y body axes resulted in angular accelerations of almost $1^{o}/sec^{2}$ at a lunar T/W of 1.0, which precluded effective pilot control with an acceleration-command system.

(2) The rate deadband of the rate-command system should not exceed 0.4^{o}/sec, and 0.2^{o}/sec is desirable.

(3) Angular acceleration capabilities of approximately $15^{o}/sec^{2}$ to $20^{o}/sec^{2}$ in pitch and roll and $10^{o}/sec^{2}$ in yaw are desirable.

(4) A throttle sensitivity of about $0.04g_{m}$ per degree of throttle deflection is desirable for altitude control during near-hover maneuvers.

These control characteristics were employed in the remaining flights conducted during the investigation. In addition, the pilots felt that although an altimeter may not be absolutely necessary for the flight vehicle, it is desirable and was generally included.

The results of the low-altitude phase of the investigation are presented in the following table in the form of the arithmetic mean and standard deviation from the mean of the touchdown conditions for a total of 139 flights:

Parameter	Arithmetic mean	Standard deviation	Arithmetic mean	Standard deviation
	0.2^{o}/sec rate deadband		0.4^{o}/sec rate deadband	
V_V, ft/sec (m/sec) . . .	-4.88 (-1.48)	2.47 (0.75)	-5.63 (-1.72)	2.78 (0.85)
V_H, ft/sec (m/sec) . . .	3.53 (1.07)	2.14 (0.65)	2.83 (0.86)	1.69 (0.51)
S, ft (m)	106.1 (32.3)	32.3 (9.8)	84.0 (25.6)	80.1 (24.4)
p, deg/sec	-0.01	0.17	0.15	0.12
q, deg/sec	0.01	0.21	-0.10	0.14
r, deg/sec	0.004	0.09	-0.03	0.25
θ, deg	-0.42	0.93	-0.49	1.45
ϕ, deg	0.50	1.30	1.23	0.98

The pilots landed within 150 feet (45.7 meters) of the desired landing site with touchdown velocities generally less than 8 ft/sec (2.4 m/sec) vertically and 6 ft/sec (1.8 m/sec) horizontally when using the 0.2°/sec rate deadband. Although the touchdown conditions attained using the 0.4°/sec rate deadband are comparable, the pilots much preferred the tighter deadband. This preference occurs primarily because the vehicle had a tendency to drift off the desired approach during final descent with the 0.4°/sec rate deadband, and thus required considerable monitoring of the three-axis gyro-horizon for precise attitude control. The velocity components at touchdown for the individual flights are presented in figure 5.

Long-Range Flights

The data attained for the 2.25 n. mi. (4.167 km) range flights, using the 1200:1 scale model, were basically the same for all the pilots. However, only one pilot, a research engineer, performed a sufficient number of flights with a given configuration for the data to be statistically significant and only his data are presented. The performance of the remaining pilots is discussed individually only when it differs from that of the primary pilot.

Flights using basic instrumentation.- The initial 2.25 n. mi. (4.167 km) range flights were performed by using a rate-command attitude control system with either a 0.2°/sec or a 0.4°/sec rate deadband. The results of a typical flight performed with the 0.2°/sec rate deadband are presented in figure 6. The time history shows that the pilot was unable to maintain the desired 500-foot (152.4-meter) flat-top trajectory with the altitude varying between about 500 feet (152.4 meters) and 1000 feet (304.8 meters). The pilots generally gained altitude during the deceleration phase while they were concentrating on bringing the translational velocities to nearly zero above the desired landing site. Although the reaction control jets for pitch and roll control appear to be very near a limit cycle with the 0.2°/sec deadband and 0.0067-foot (0.002-meter) center-of-gravity offsets, less than 0.2 slug (2.9 kg) of reaction-control-system fuel are required during a 2.25 n. mi. (4.167 km) trajectory. Increasing the rate deadband to 0.4°/sec reduced the reaction-control-system activity (fig. 7) but was considered to be less desirable by the pilots.

The results of this phase of the investigation are presented in the following table in the form of the arithmetic mean and the standard deviation from the mean of the touchdown conditions for a total of 87 flights:

Parameter	Arithmetic mean	Standard deviation	Arithmetic mean	Standard deviation
	0.2^{o}/sec rate deadband		0.4^{o}/sec rate deadband	
V_V, ft/sec (m/sec) . . .	-20.49 (-6.24)	7.88 (2.40)	-16.26 (-4.96)	8.11 (2.47)
V_H, ft/sec (m/sec) . . .	7.18 (2.19)	3.87 (1.18)	7.88 (2.40)	4.36 (1.33)
S, ft (m)	237.9 (72.5)	190.5 (58.1)	306.1 (93.3)	174.6 (53.2)
p, deg/sec	0.15	0.77	0.20	1.58
q, deg/sec	0.03	0.20	-0.35	1.21
r, deg/sec	0.13	0.09	0.02	0.27
θ, deg	-0.73	0.85	-0.92	1.81
ϕ, deg	0.13	1.00	0.81	1.54
ΔV, ft/sec (m/sec) . . .	1197.6 (365.0)	199.0 (60.6)	1263.8 (385.2)	153.1 (46.7)
Flight time, sec	209.1	38.1	222.1	28.5
Hover time, sec	76.4	29.0	96.5	23.9

It should be noted that although these terminal conditions were obtained at zero altitude, the scene generation equipment of the simulator ceased operating at an altitude of 150 feet (45.7 meters). The touchdown velocities and miss distances are consequently larger than was experienced in the preliminary investigation in which the simulator operated all the way to touchdown. The tendency of the vehicle attitudes to drift with the 0.4^{o}/sec deadband was particularly objectionable during final descent and contributed to the increase in miss distance over that experienced with the 0.2^{o}/sec deadband. Additional time at near-hover conditions during descent was required with the larger deadband and resulted in an increase in the required characteristic velocity. The location of the landing sites chosen by the pilot relative to the 340-foot-diameter (103.6-meter) crater that defined the desired landing area are shown in figure 8.

These results are, in general, typical of those of all the participating pilots, with two exceptions. The second research engineer was very cautious in descending and required an average of approximately 2 minutes at near-hover conditions with a resulting characteristic velocity that averaged 1448.1 ft/sec (441.38 m/sec) for 18 flights. In addition, one of the research pilots objected to the requirement of bringing his translational velocities to nearly zero at altitudes greater than 150 feet (45.7 meters) because he would normally do so at lower altitudes. This research pilot's performance, however, did not differ significantly from that of the other pilots.

Flights using horizontal- and vertical-velocity indicators.- In order to determine whether the pilots performance could be improved if vertical- and horizontal-velocity information were available, a number of flights were performed with velocity indicators included and with a rate-command deadband of 0.2^{o}/sec. The results of a typical piloted flight are presented in figure 9. The pilot's performance in maintaining the 500-foot altitude (152.4-meter) flat-top trajectory was generally improved over the flights performed without vertical-velocity information, although the vehicle still gained some altitude during deceleration.

A total of 38 flights were performed by the primary pilot using the velocity indicators. The arithmetic mean and standard deviation from the mean at touchdown are presented in the following table:

Parameter	Arithmetic mean	Standard deviation
	0.2^{o}/sec rate deadband	
V_V, ft/sec (m/sec) . . .	-10.97 (-3.34)	3.39 (1.03)
V_H, ft/sec (m/sec) . . .	4.06 (1.24)	2.69 (0.82)
S, ft (m)	254.8 (77.7)	126.7 (38.6)
p, deg/sec	-0.07	0.66
q, deg/sec	-0.11	0.51
r, deg/sec	0.04	0.09
θ, deg	-0.01	0.71
ϕ,deg	0.30	0.55
ΔV, ft/sec (m/sec) . . .	1054.1 (321.3)	92.2 (28.1)
Flight time	174.5	17.4
Hover time	66.7	15.4

The most significant effect of adding horizontal- and vertical-velocity indicators was to decrease the average characteristic velocity requirement by approximately 150 ft/sec (45.7 m/sec) and the standard deviation by about 100 ft/sec (30.5 m/sec). In addition, the pilots were able to avoid overshooting the desired landing site when velocity indicators were included and, in general, landed short of the target crater (fig. 10) and

thus contributed to a reduction in total flight time. Velocity information appears to be desirable from a piloting standpoint; however, weight considerations may preclude its incorporation.

Flights without velocity or altitude indicators.- It was believed that the previous experience in flying the 2.25 n. mi. (4.167 km) flat-top trajectory early in the study would enable the pilots to perform satisfactorily without either altitude or velocity information. The primary pilot consequently performed a total of 35 flights without an altimeter or velocity indicators by using a rate-command control system with a 0.2°/sec deadband. Four of the flights resulted in crashes during the deboost phase of the maneuver when the vehicle was pitched to an angle of 45°. Part of the difficulty in judging altitude during deceleration was associated with the 90° by 90° field of view of the simulation equipment. The narrow field of view resulted in a very poor view of the lunar surface when the vehicle was pitched to 45°, this condition would not exist with an actual vehicle. The results of the 31 successful flights are presented in the following table in the form of the arithmetic mean and standard deviation from the mean at touchdown:

Parameter	Arithmetic mean	Standard deviation
	0.2°/sec rate deadband	
V_V, ft/sec (m/sec) . . .	-12.65 (-3.86)	3.78 (1.15)
V_H, ft/sec (m/sec) . . .	5.04 (1.54)	3.26 (0.99)
S, ft (m)	217.9 (66.4)	210.8 (64.2)
p, deg/sec	-0.05	0.30
q, deg/sec	-0.11	0.63
r, deg/sec	0.04	0.10
θ, deg	0.001	0.61
ϕ, deg	0.42	0.50
ΔV, ft/sec (m/sec) . . .	1162.5 (354.3)	167.9 (51.2)
Flight time, sec	204.0	33.4
Hover time, sec	72.9	24.8

The location of the landing sites chosen by the pilot relative to the target crater are shown in figure 11. The touchdown conditions, particularly, miss distance and characteristic velocity requirements, obtained without an altimeter are very similar to those presented in the first table for flights performed with an altimeter. It should be emphasized, however, that the pilot was extremely well trained in performing the nominal 2.25 n. mi. (4.167 km) range flat-top trajectory when the flights were made without the altimeter. Based on their previous experience, the pilots knew that their altitude would be very nearly 500 feet (152.4 meters) at the beginning of the acceleration phase. Knowing the approximate altitude at this point, the pilots were able to judge changes in altitude, rather than altitude itself, sufficiently well to approximate the 500-foot-altitude (152.4-meter) flat-top trajectory. (See fig. 12.) On those occasions that the pilots inadvertantly permitted altitude to exceed 1000 feet (304.8 meters) during deceleration, extreme difficulty was experienced in judging altitude changes and vehicle velocities. It is, therefore, believed that the higher the altitude the greater the need for an altimeter in order to perform the maneuver.

In order to examine the pilot's performance with completely unknown initial altitudes and velocities, 10 flights were initiated at random low altitudes above the normal landing site and the pilots attemped to fly back to the normal take-off point. The pilots experienced difficulty in judging altitude and vertical velocity during the acceleration phase at a pitch angle of -45°. Two of the first three flights crashed and although the remaining flights were successful, the maximum altitudes reached were between 1200 feet (365.8 meters) and 1800 feet (548.6 meters); as a result the flights were performed rather inefficiently.

Effect of Cruise Velocity

Without piloting errors there is a near-optimal cruise velocity (ref. 2) of approximately 200 ft/sec (60.96 m/sec) for a 2.25 n. mi. (4.167 km) range flat-top trajectory using a lunar T/W of 1.4 and a 45° pitch angle during the acceleration and deceleration phases. The pilots however were not required to employ a particular cruise velocity and generally translated at velocities between 100 ft/sec (30.5 m/sec) and 250 ft/sec (76.2 m/sec). The arithmetic mean and standard deviation from the mean of hover time, characteristic velocity, and cruise velocity are presented in the following table for the flights performed using the basic instrumentation and a rate-command attitude-control system with a 0.2°/sec rate deadband:

Parameter	Arithmetic mean	Standard deviation	Number of runs
$V_{H,c} \leqq 140$ ft/sec ($V_{H,c} \leqq 42.8$ m/sec)			
$V_{H,c}$	126.3 ft/sec (38.5 m/sec)	11.6 ft/sec (3.5 m/sec)	12
Hover time	80.9 sec	33.7 sec	12
ΔV	1196.1 ft/sec (364.6 m/sec)	194.4 ft/sec (59.2 m/sec)	12
140 ft/sec < $V_{H,c}$ < 160 ft/sec (42.8 m/sec < $V_{H,c}$ < 48.8 m/sec)			
$V_{H,c}$	147.9 ft/sec (45.1 m/sec)	4.3 ft/sec (1.3 m/sec)	9
Hover time	74.7 sec	31.9 sec	9
ΔV	1145.2 ft/sec (349.0 m/sec)	176.9 ft/sec (53.9 m/sec)	9
160 ft/sec $\leqq V_{H,c} \leqq$ 170 ft/sec (48.8 m/sec $\leqq V_{H,c} \leqq$ 51.8 m/sec)			
$V_{H,c}$	163.9 ft/sec (49.9 m/sec)	4.3 ft/sec (1.3 m/sec)	11
Hover time	67.7 sec	24.2 sec	11
ΔV	1091.5 ft/sec (332.7 m/sec)	139.4 ft/sec (42.5 m/sec)	11
$V_{H,c}$ > 170 ft/sec ($V_{H,c}$ > 51.8 m/sec)			
$V_{H,c}$	185.3 ft/sec (56.5 m/sec)	20.0 ft/sec (6.1 m/sec)	7
Hover time	86.1 sec	26.8 sec	7
ΔV	1214.4 ft/sec (370.1 m/sec)	140.9 ft/sec (42.9 m/sec)	7

When the basic instrumentation was employed, the average cruise velocity for all flights was 152.8 ft/sec (46.6 m/sec). The most efficient flights, however, were performed with a cruise velocity of 160 ft/sec (48.8 m/sec) to 170 ft/sec (51.8 m/sec). When cruise velocities in excess of 170 ft/sec (51.8 m/sec) were employed, the pilots experienced difficulty in completing the deceleration phase of the maneuver near the desired landing site. Consequently, the pilots had to spend considerably more time at near-hover conditions in order to attain acceptable miss distances at touchdown and as a result, there was an increase in the required characteristic velocity.

The average cruise velocity employed by the pilot varied considerably with the instrumentation used. When vertical- and horizontal-velocity indicators were included, the average cruise velocity was 173.8 ft/sec (53.0 m/sec). The time spent at near-hover conditions did not increase for cruise velocities in excess of 170 ft/sec (51.8 m/sec) when the velocity indicators were employed and the characteristic velocity requirements remained relatively small.

When the pilot was required to fly without velocity indicators or an altimeter, he became rather cautious and as a result, had an average cruise velocity of 132.8 ft/sec (40.5 m/sec). Although cruise velocity affects the characteristic velocity requirements, the time spent during descent at near-hover conditions is the primary factor affecting fuel expenditure.

CONCLUDING REMARKS

A fixed-base visual-simulation study has been conducted to determine the control characteristics and instrumentation necessary for a pilot to operate a lunar flying vehicle efficiently. The simulation included six rigid-body degrees of freedom of the vehicle. The basic instrumentation used consisted of a three-axis gyro-horizon, a lunar thrust-weight ratio indicator, a fuel indicator, and an altimeter.

The purpose of the initial phase of the investigation was to determine, within the limits of the fixed-base simulation, the vehicle handling qualities necessary for efficient operation. The pilot's task was to ascend to an altitude of about 150 feet (45.7 meters), translate a few hundred feet, and land. Subject to the limitations imposed by the fixed-base simulation, it was concluded that: (1) the minimum acceptable attitude control system for center-of-gravity offsets on the order of 0.0067 foot (0.002 meter) was a rate-command system; (2) the rate deadband of the rate-command system should not exceed 0.4°/sec (0.2°/sec is desirable); (3) attitude control power should be between $10^{\circ}/sec^2$ and $20^{\circ}/sec^2$ about all axes; and (4) main-engine throttle sensitivity of about 0.04 lunar g per degree of throttle deflection is desirable. With these control characteristics, the pilots generally landed within approximately 150 feet (45.7 meters) of the desired landing site with touchdown velocities of less than 8 ft/sec (2.4 m/sec) vertically and 6 ft/sec (1.8 m/sec) horizontally.

The purpose of the second phase of the investigation was to determine the instrumentation and control requirements for flying 500-foot-altitude (152.4-meter) trajectories over a range of 2.25 n. mi. (4.167 km). The pilot's task was to fly the 500-foot-altitude (152.4-meter) flat-top trajectory near a specified crater, bring the translational velocity components to nearly zero at an altitude of approximately 150 feet (45.7 meters) (a simulator restriction), and descend to the lunar surface. When the basic instrumentation which included an altimeter was used, the simulated flights required an average characteristic velocity of 1197.6 ft/sec (365.0 m/sec) with a standard deviation of 199.0 ft/sec (60.6 m/sec). When horizontal and vertical velocity indicators were added, the average characteristic velocity was reduced by approximately 150 ft/sec (45.7 m/sec) and the standard deviation by about 100 ft/sec (30.5 m/sec). This improvement was primarily due to a reduction in time spent at near-hover conditions while acquiring and descending to the desired landing site. Flights performed without the benefit of either an altimeter or

velocity indicators required approximately the same characteristic velocity as flights performed with an altimeter. It should be emphasized that only an extremely well-trained pilot, familiar with the nominal flight profile, could adequately perform the maneuver without an altimeter. It is believed that as the vehicle altitude increases above about 1000 feet (304.8 meters), the need for an altimeter also increases. The translational or cruise velocity employed by the pilots varied considerably with the instrumentation, the highest velocities being successfully employed when the velocity indicators were present. When the basic instrumentation was used, the flights made with cruise velocities of 160 ft/sec (48.8 m/sec) to 170 ft/sec (51.8 m/sec) resulted in the smallest expenditure of fuel. The use of higher velocities usually required additional time to attain acceptable miss distances with correspondingly greater fuel expenditure. Although the vehicle was capable of a lunar thrust-weight ratio of 3.0 with the vehicle fully loaded, the pilots never exceeded 1.8.

Langley Research Center,
National Aeronautics and Space Administration,
Hampton, Va., August 5, 1970.

APPENDIX A

SYMBOLS

Measurements for this investigation were made in the U.S. Customary Units but are also given in the International System of Units (SI). (See ref. 4.) Transformation matrices for the assumed axis systems are presented in appendix B.

A_{ij}	direction cosines ($i = 1, 2, 3$; $j = 1, 2, 3$)
a	distance from geometrical center of lunar flying vehicle to reaction control jets, 3.33 ft (1.01 m)
b,c,d,e	quaternions or Euler parameters (ref. 5)
f_i	reaction control thrust ($i = 1, \ldots 6$ where f_1 and f_2 provide roll control, f_3 and f_4 provide pitch control, and f_5 and f_6 provide yaw control)
g_e	acceleration due to gravitational attraction at surface of earth, 32.2 ft/sec^2 (9.82 m/sec^2)
g_m	acceleration due to gravitational attraction at surface of moon, 5.32 ft/sec^2 (1.62 m/sec^2)
h	altitude above lunar surface, ft (m)
I_{sp}	specific impulse, 300 sec
I_X, I_Y, I_Z	moments of inertia about vehicle body axes, slug-ft^2 (kg-m^2)
m	vehicle mass, slugs (kg)
p,q,r	vehicle angular velocities about X, Y, and Z body axes, respectively, radians/sec or deg/sec
R_m	assumed radius of moon, 5.702086×10^6 ft (1.737996×10^6 m)
R, Ψ, Y_i	cylindrical coordinate system with origin at center of moon and vector R and angle Ψ in X_iY_i-plane (see fig. 13)

S miss distance defined as range between actual and desired landing points, ft (m)

T main engine thrust through geometrical center of vehicle positive in negative Z-direction, lb (N) (see fig. 14)

T/W lunar thrust-weight ratio, $\frac{T}{mg_m}$

t time, sec

ΔV characteristic velocity, $g_e I_{sp} \log_e \frac{m_o}{m}$, ft/sec (m/sec)

V_H horizontal-velocity component, ft/sec (m/sec)

$V_{H,c}$ horizontal velocity during translation, referred to as cruise velocity, ft/sec (m/sec)

V_V vertical velocity component, ft/sec (m/sec)

W vehicle lunar weight, mg_m, lb (N)

X,Y,Z orthogonal reference coordinate system with origin at center of gravity of lunar flying vehicle, referred to as body axes (see fig. 13)

X_c,Y_c,Z_c moving-reference coordinate system with origin at surface of moon and with Z_c-axis alined with local vertical and positive inward, X_c-axis positive westward and Y_c-axis positive northward (see fig. 13)

X_i,Y_i,Z_i fixed-reference coordinate system with origin located at center of moon (see fig. 13)

X_{op},Y_{op},Z_{op} optics coordinate system with origin at center of gravity of vehicle, differs from body axis by angle θ_{op} (see fig. 13)

δ_T rocket-throttle-control displacement, radians or deg

ϵ_X,ϵ_Y horizontal displacements of vehicle thrust vector, along the X- and Y-axes, from the vehicle center of gravity (see fig. 14), ft (m)

ϵ_Z center-of-gravity displacement along Z-axis due to fuel consumption (see figs. 1 and 13), ft (m)

λ direction of flight referenced to north, defined as angle between V_H and Y_C axis, deg

θ_{op} angle of optical axis of viewing system in X,Z-plane, measured from X-axis, deg

ψ, θ, ϕ Euler angles of rotation relating body axes and fixed-reference system, radian or deg

$\{\}$ column matrix

$[\,]$ square matrix

$[\,]^T$ transpose of matrix

$\left[\Gamma_{m,n}\right]_{\substack{m=B,C,I,O \\ n=B,C,I,O}}$ matrix which transforms a vector from axis system m to axis system n; B, C, I, and O represent body system, moving-reference system, fixed-reference system, and optics system, respectively

Subscript:

o initial conditions

A dot over a symbol indicates a time derivative.

APPENDIX B

FORMULATION OF EQUATIONS OF MOTION

Force Equations

The equations of motion for the three translational degrees of freedom are written in the cylindrical-axis system:

$$\ddot{R} - R\dot{\Psi}^2 = -\frac{F_{Z_c}}{m} - g_m\left(\frac{R_m}{R}\right)^2 \tag{B1}$$

$$R\ddot{\Psi} + 2\dot{R}\dot{\Psi} = \frac{F_{X_c}}{m} \tag{B2}$$

$$\ddot{Y}_i = \frac{F_{Y_c}}{m} \tag{B3}$$

where F_{X_c}, F_{Y_c}, and F_{Z_c} are the forces along the X_c-, Y_c-, and Z_c-axis, respectively, and are given by

$$\begin{Bmatrix} F_{X_c} \\ F_{Y_c} \\ F_{Z_c} \end{Bmatrix} = \left[\Gamma_{C,B}\right]^T \begin{Bmatrix} F_X \\ F_Y \\ F_Z \end{Bmatrix} \tag{B4}$$

where F_X, F_Y, and F_Z are the force components in the body-axis system and are given by

$$F_X = f_5 + f_6 \tag{B5}$$

$$F_Y = 0 \tag{B6}$$

$$F_Z = -\left(T + f_1 + f_2 + f_3 + f_4\right) \tag{B7}$$

and where the orthogonal matrix relating the moving-reference axis system to the body axis system is given by

$$\left[\Gamma_{C,B}\right] = \left[\Gamma_{I,B}\right]\left[\Gamma_{C,I}\right] \tag{B8}$$

where

$$\left[\Gamma_{C,I}\right] = \begin{bmatrix} \cos\Psi & 0 & -\sin\Psi \\ 0 & 1 & 0 \\ \sin\Psi & 0 & \cos\Psi \end{bmatrix} \tag{B9}$$

and

$$\left[\Gamma_{I,B}\right] = \begin{bmatrix} A_{11} & A_{12} & A_{13} \\ A_{21} & A_{22} & A_{23} \\ A_{31} & A_{32} & A_{33} \end{bmatrix} \tag{B10}$$

the direction cosines are given in terms of quaternions (ref. 5) by

$$A_{11} = 2(b^2 + e^2) - 1 \tag{B11}$$

$$A_{12} = 2(bc + de) \tag{B12}$$

$$A_{13} = 2(bd - ce) \tag{B13}$$

$$A_{21} = 2(bc - de) \tag{B14}$$

$$A_{22} = 2(c^2 + e^2) - 1 \tag{B15}$$

$$A_{23} = 2(be + cd) \tag{B16}$$

$$A_{31} = 2(bd + ce) \tag{B17}$$

$$A_{32} = 2(cd - be) \tag{B18}$$

$$A_{33} = 2(d^2 + e^2) - 1 \tag{B19}$$

and

$$\dot{b} = \frac{1}{2}(ep - dq + cr) + Kgb \tag{B20}$$

$$\dot{c} = \frac{1}{2}(dp + eq - br) + Kgc \tag{B21}$$

$$\dot{d} = \frac{1}{2}(-cp + bq + er) + Kgd \tag{B22}$$

$$\dot{e} = -\frac{1}{2}(bp + cq + dr) + Kge \tag{B23}$$

where

$$g = 1 - (b^2 + c^2 + d^2 + e^2) \tag{B24}$$

and K is a gain factor determined empirically on the computer.

Moment Equations

The equations of motion for the three rotational degrees of freedom are written in the body-axis system:

$$\dot{p} = \frac{1}{I_X}\left[(f_1 - f_2)a + (T + f_1 + f_2 + f_3 + f_4)\epsilon_Y + (I_Y - I_Z)qr\right] \tag{B25}$$

$$\dot{q} = \frac{1}{I_Y}\left[(f_3 - f_4)a - (T + f_1 + f_2 + f_3 + f_4)\epsilon_X - (f_5 + f_6)\epsilon_Z + (I_Z - I_X)pr\right] \tag{B26}$$

$$\dot{r} = \frac{1}{I_Z}\left[(f_5 - f_6)a + (f_5 + f_6)\epsilon_Y + (I_X - I_Y)pq\right] \tag{B27}$$

Auxiliary Equations

The matrix which transforms a vector from the moving-reference axis system to the optics-axis system is given by

$$\left[\Gamma_{C,O}\right] = \begin{bmatrix} \gamma_{11} & \gamma_{12} & \gamma_{13} \\ \gamma_{21} & \gamma_{22} & \gamma_{23} \\ \gamma_{31} & \gamma_{32} & \gamma_{33} \end{bmatrix} = \left[\Gamma_{B,O}\right]\left[\Gamma_{C,B}\right] \tag{B28}$$

where

$$\left[\Gamma_{B,O}\right] = \begin{bmatrix} \cos\theta_{op} & 0 & \sin\theta_{op} \\ 0 & 1 & 0 \\ -\sin\theta_{op} & 0 & \cos\theta_{op} \end{bmatrix} \tag{B29}$$

and where γ_{ij} are direction cosines relating the optics-axis system to the moving-reference axis system (i = 1, 2, 3; j = 1, 2, 3). Thus, the angles $\bar{\psi}$, $\bar{\theta}$, and $\bar{\phi}$ used to drive the optical pickup are given by

$$\left.\begin{aligned} \sin\bar{\theta} &= -\gamma_{13} \\ \cos\bar{\theta} &+ \sqrt{1-(\gamma_{13})^2} \end{aligned}\right\} \qquad \left(-\frac{\pi}{2} < \theta < \frac{\pi}{2}\right) \tag{B30}$$

$$\left.\begin{aligned} \sin\bar{\phi} &= \frac{\gamma_{23}}{\cos\bar{\theta}} \\ \cos\bar{\phi} &= \frac{\gamma_{33}}{\cos\bar{\theta}} \end{aligned}\right\} \tag{B31}$$

$$\left.\begin{aligned} \sin\bar{\psi} &= \frac{\gamma_{12}}{\cos\bar{\theta}} \\ \cos\bar{\psi} &= \frac{\gamma_{11}}{\cos\bar{\theta}} \end{aligned}\right\} \tag{B32}$$

The horizontal-velocity component of the vehicle is given by

$$V_H = \sqrt{\dot{X}_c^2 + \dot{Y}_c^2} \tag{B33}$$

and the vertical-velocity component by

$$V_V = -\dot{Z}_c \tag{B34}$$

where

$$\left.\begin{aligned} \dot{X}_c &= R\dot{\Psi} \\ \dot{Y}_c &= \dot{Y}_i \\ \dot{Z}_c &= -\dot{R} \end{aligned}\right\} \tag{B35}$$

Altitude is given by

$$\left.\begin{aligned} h &= R - 5\ 702\ 086 \text{ (feet)} \\ h &= R - 1\ 737\ 996 \text{ (meters)} \end{aligned}\right\} \tag{B36}$$

and characteristic velocity is given by

$$\Delta V = g_e I_{sp} \log_e \frac{m_o}{m} \tag{B37}$$

where

$$m = m_o + \int_0^t \left(\dot{m}_T + \dot{m}_f\right) dt \tag{B38}$$

with the main engine propellant flow rate given by

$$\dot{m}_T = -\frac{T}{g_e I_{sp}} \tag{B39}$$

and the reaction control system propellant flow rate given by

$$\dot{m}_f = -\frac{1}{g_e I_{sp}} \sum_{i=1}^{6} f_i \tag{B40}$$

REFERENCES

1. O'Bryan, Thomas C.; and Hewes, Donald E.: Operational Features of the Langley Lunar Landing Research Facility. NASA TN D-3828, 1967.

2. Anon: Study of One-Man Lunar Flying Vehicle. Vol. II – Mission Analysis. SD 69-419-2 (Contract NAS 9-9045), North Amer. Rockwell Space Div., Aug. 31, 1969.

3. Kaestner, P. T.: An Articulated Optical Pickup for Scale Model Simulation. J. SMPTE, vol. 76, No. 10, Oct. 1967, pp. 988-981.

4. Mechtly, E. A.: The International System of Units – Physical Constants and Conversion Factors. NASA SP-7012, 1964.

5. Robinson, Alfred C.: On the Use of Quaternions in Simulation of Rigid-Body Motion. WADC Tech. Rep. 58-17, U.S. Air Force, Dec. 1958. (Available from DDC as AD No. 234422.)

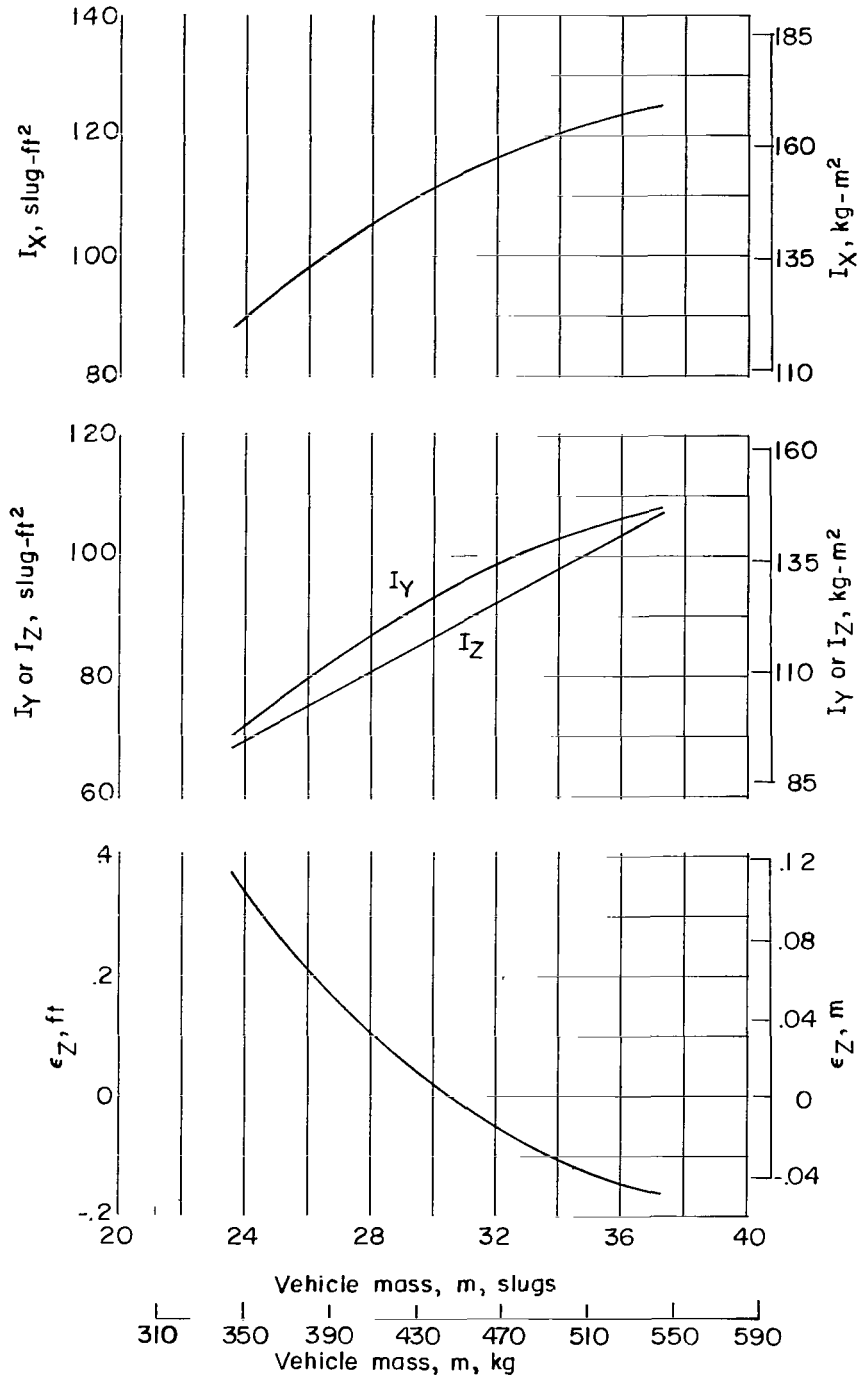

Figure 1.- Vehicle characteristics.

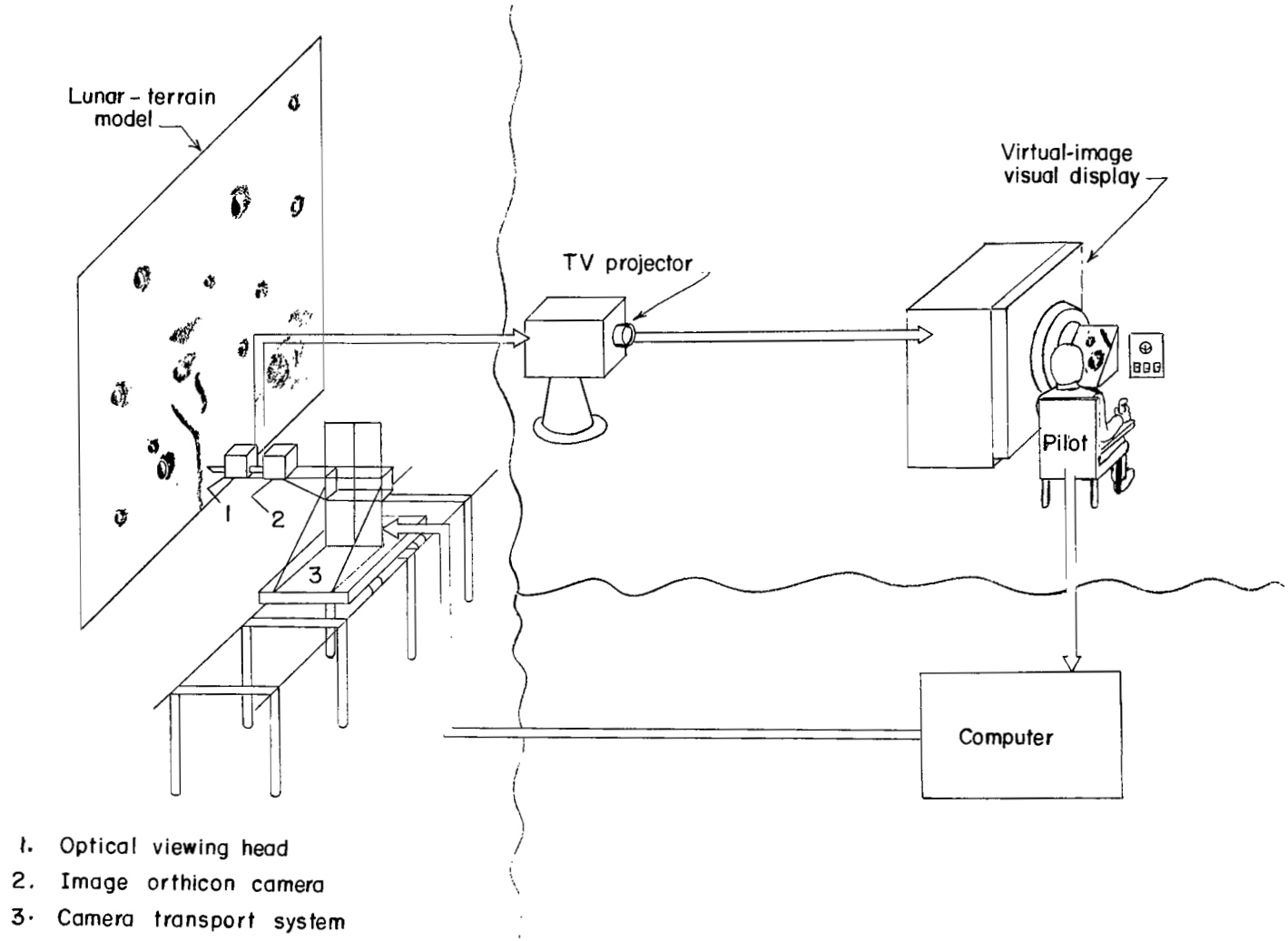

Figure 2.- Simulation equipment.

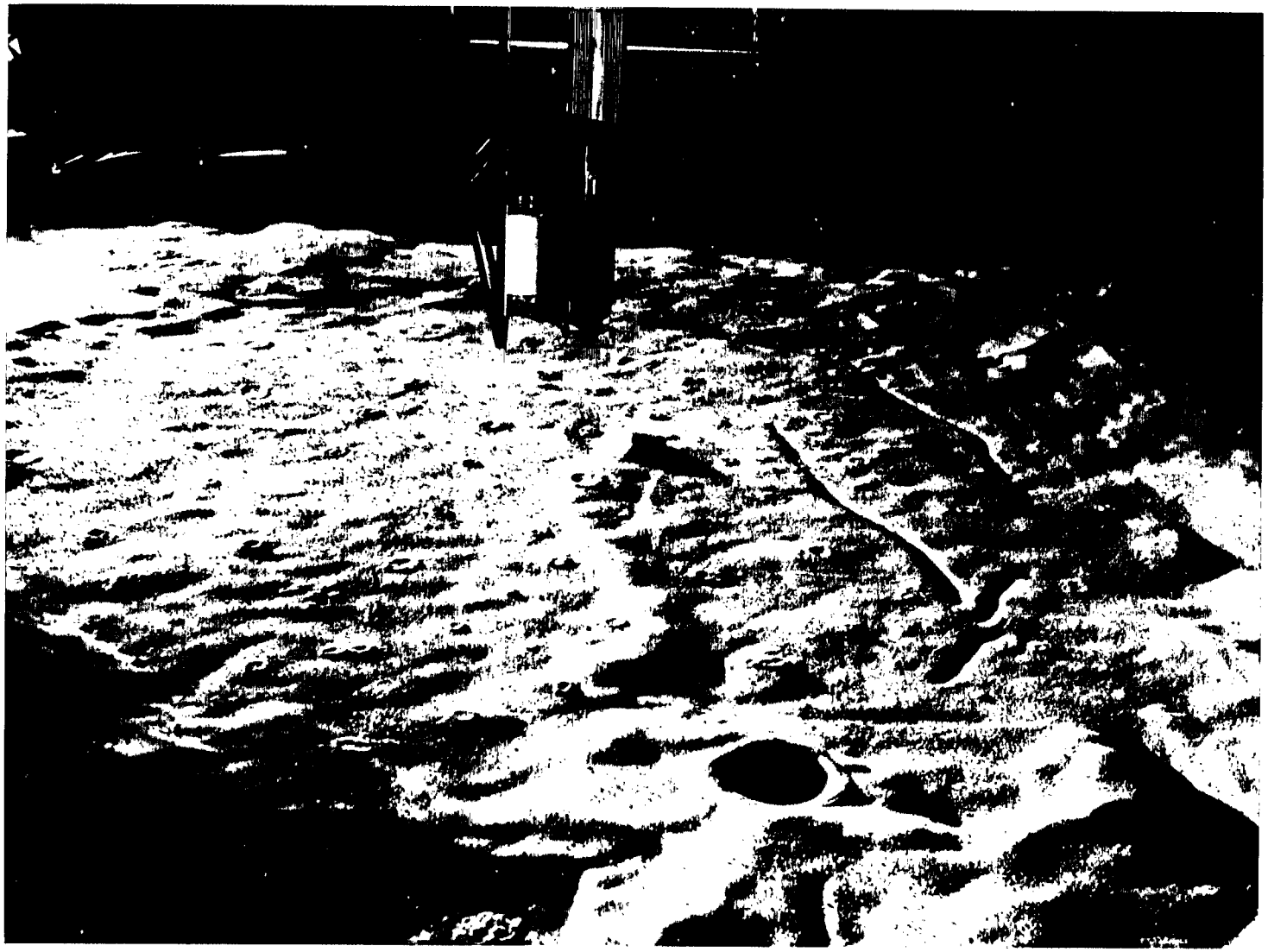

L-70-1366

Figure 3.- Lunar-terrain model and camera transport system.

L-70-1807

Figure 4.- General layout of cockpit.

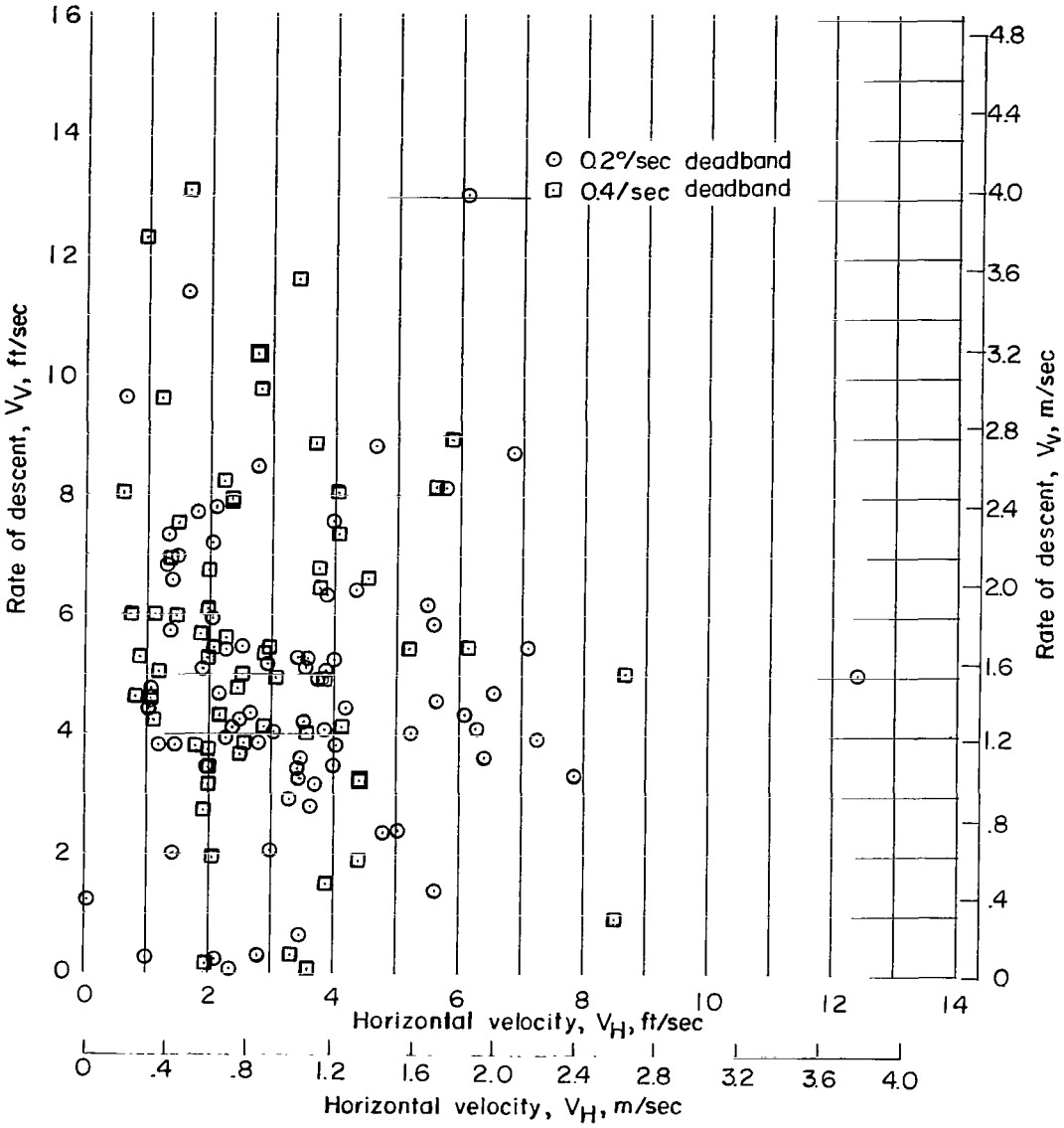

Figure 5.- Vehicle touchdown velocities.

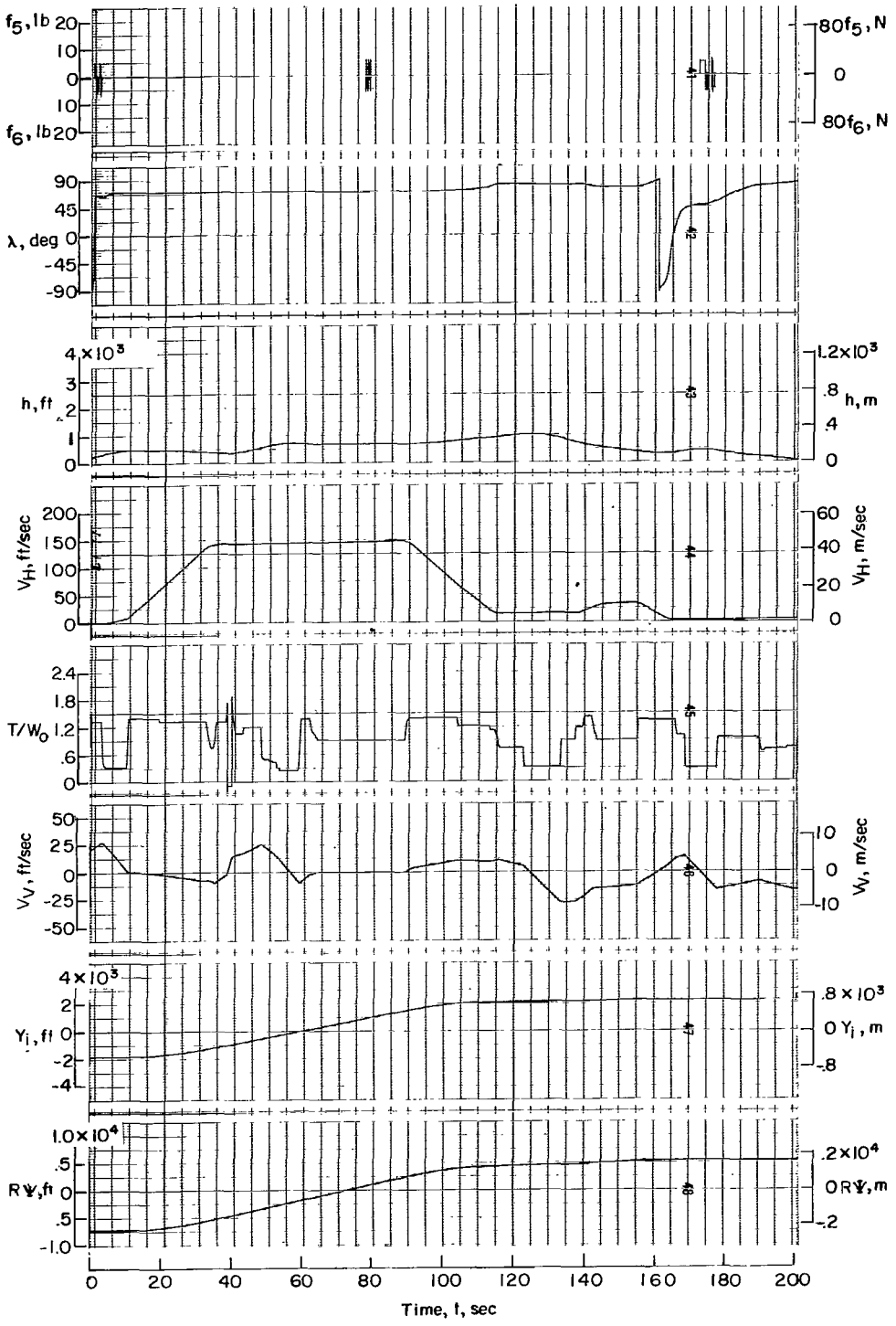

Figure 6.- Results of a typical flight performed with the basic instrumentation and a rate-command attitude control system with a 0.2°/sec rate deadband.

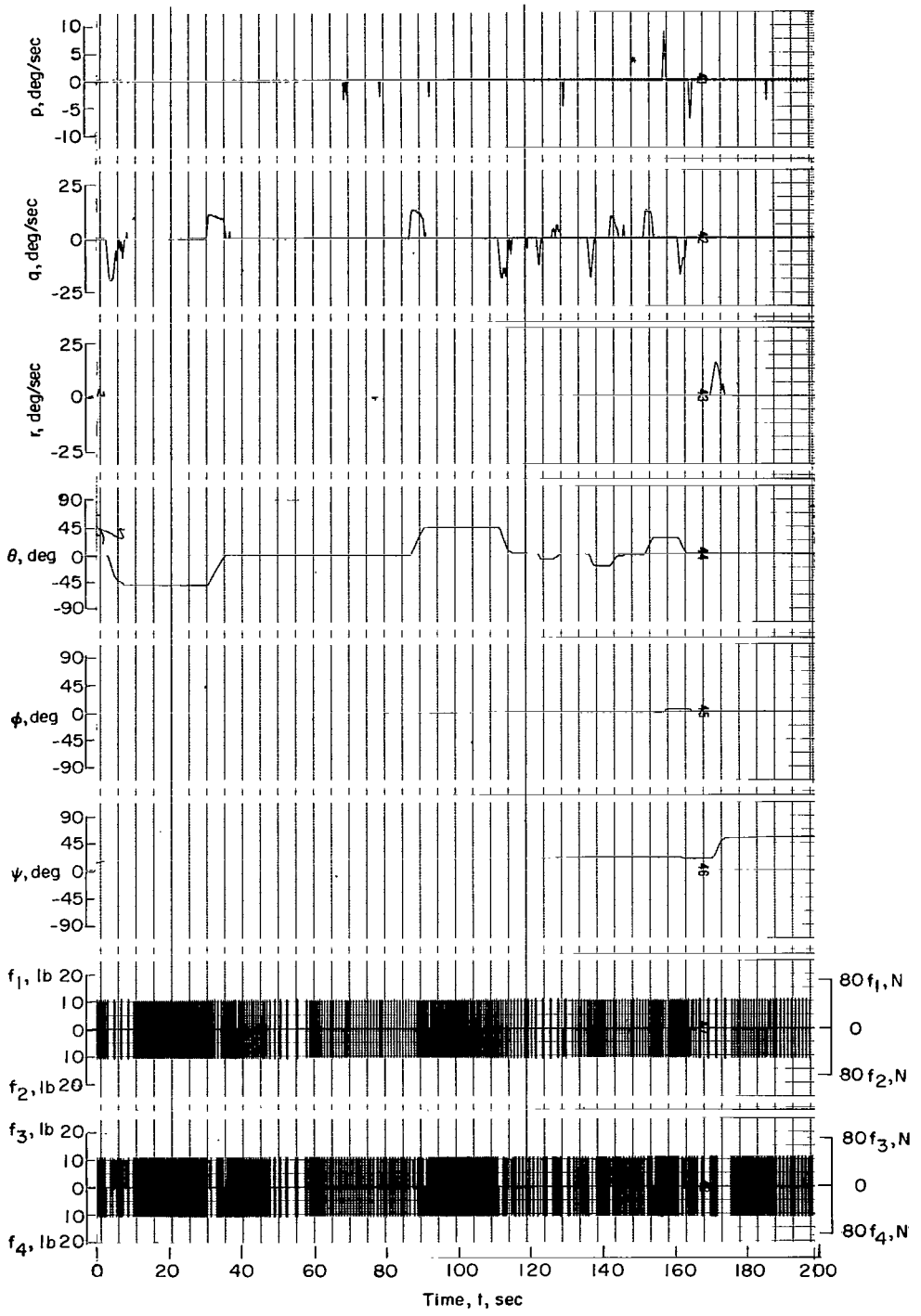

Figure 6.- Concluded.

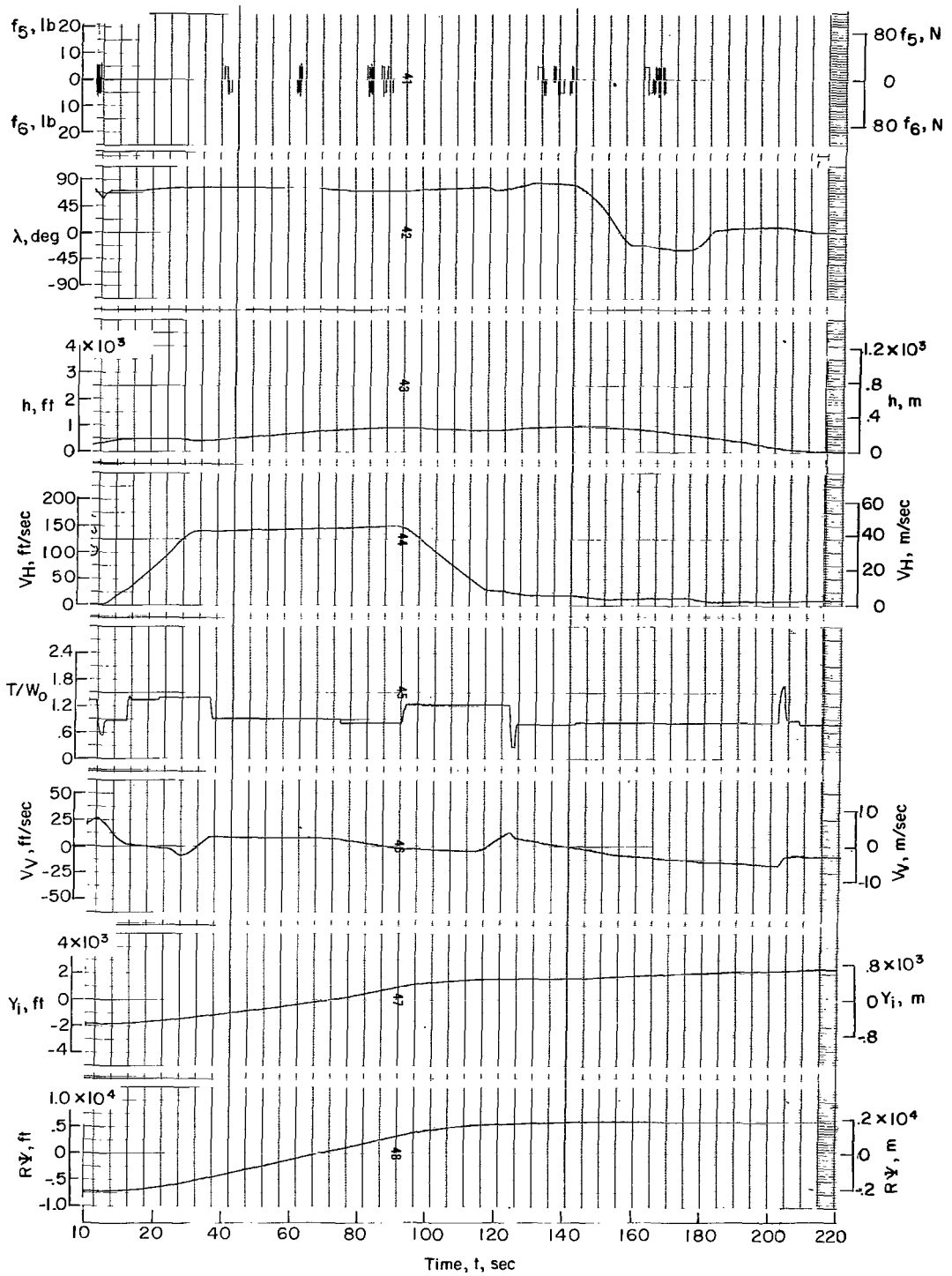

Figure 7.- Results of a typical flight performed with an altimeter and a rate-command attitude control system with a 0.4°/sec rate deadband.

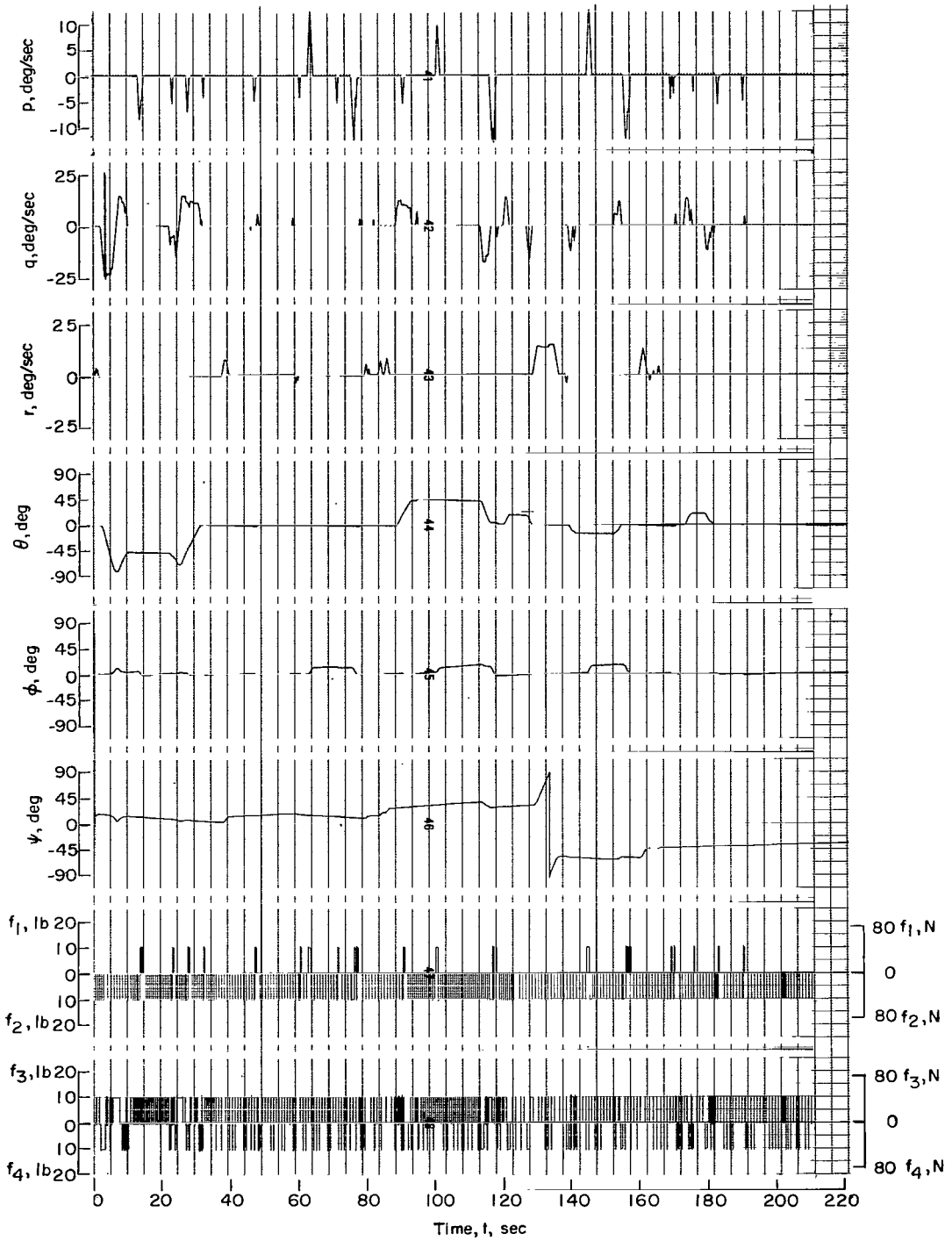

Figure 7.- Concluded.

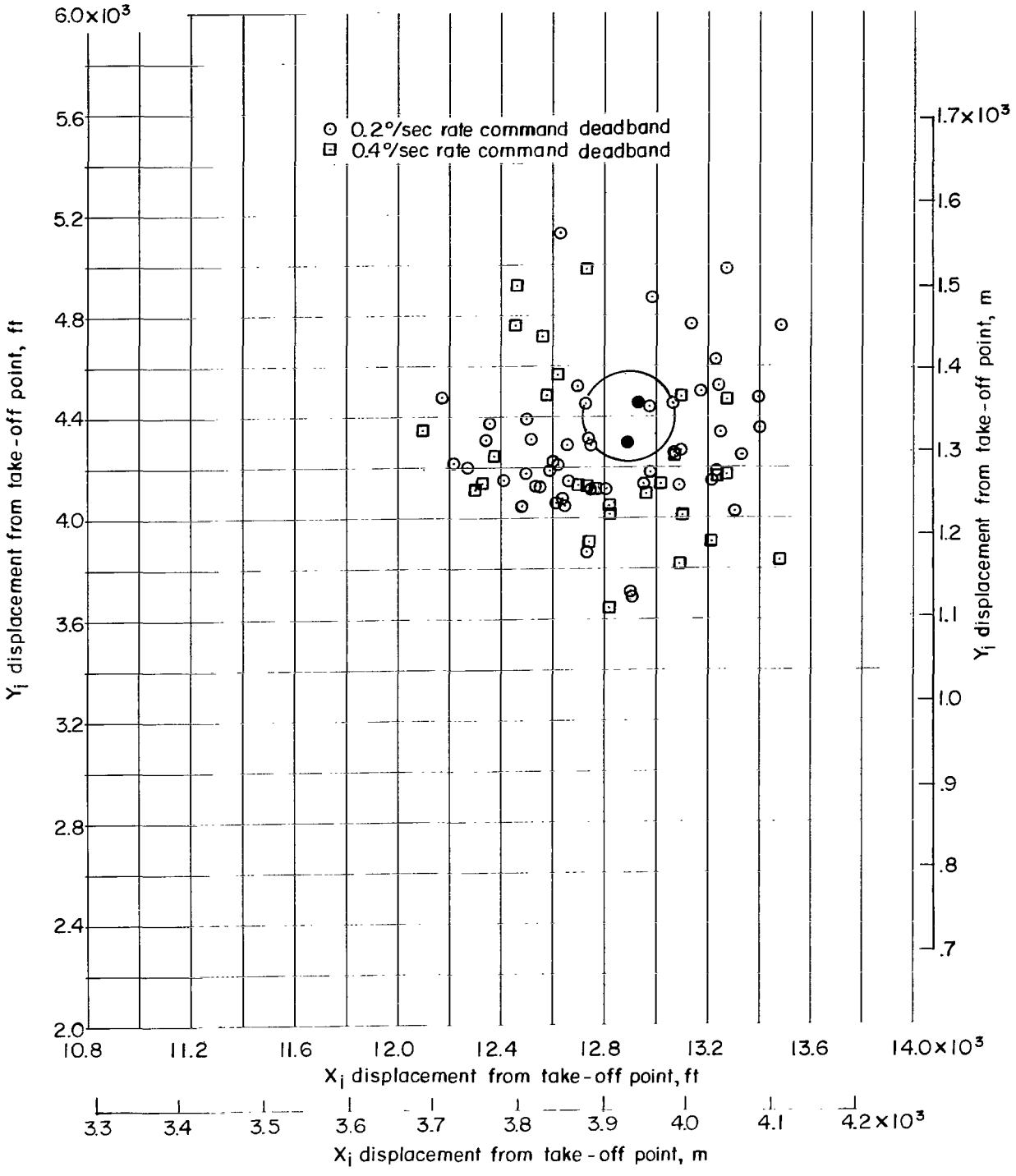

Figure 8.- Location of landing sites relative to target crater. (Shaded symbols denote flights in which pilot attempted to land inside crater.)

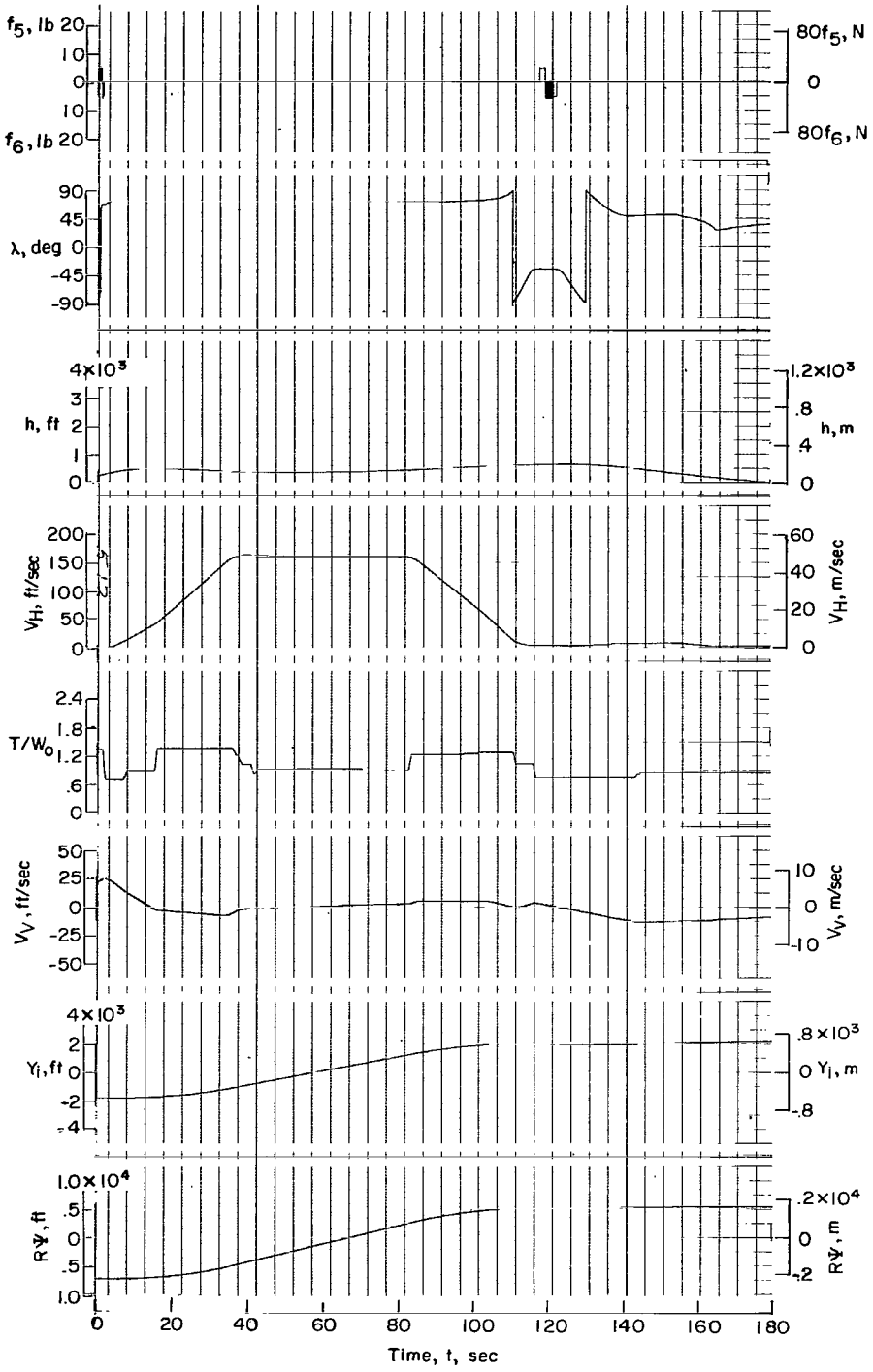

Figure 9.- Results of a typical flight using an altimeter and vertical- and horizontal-velocity indicators. (The rate deadband was 0.2°/sec.)

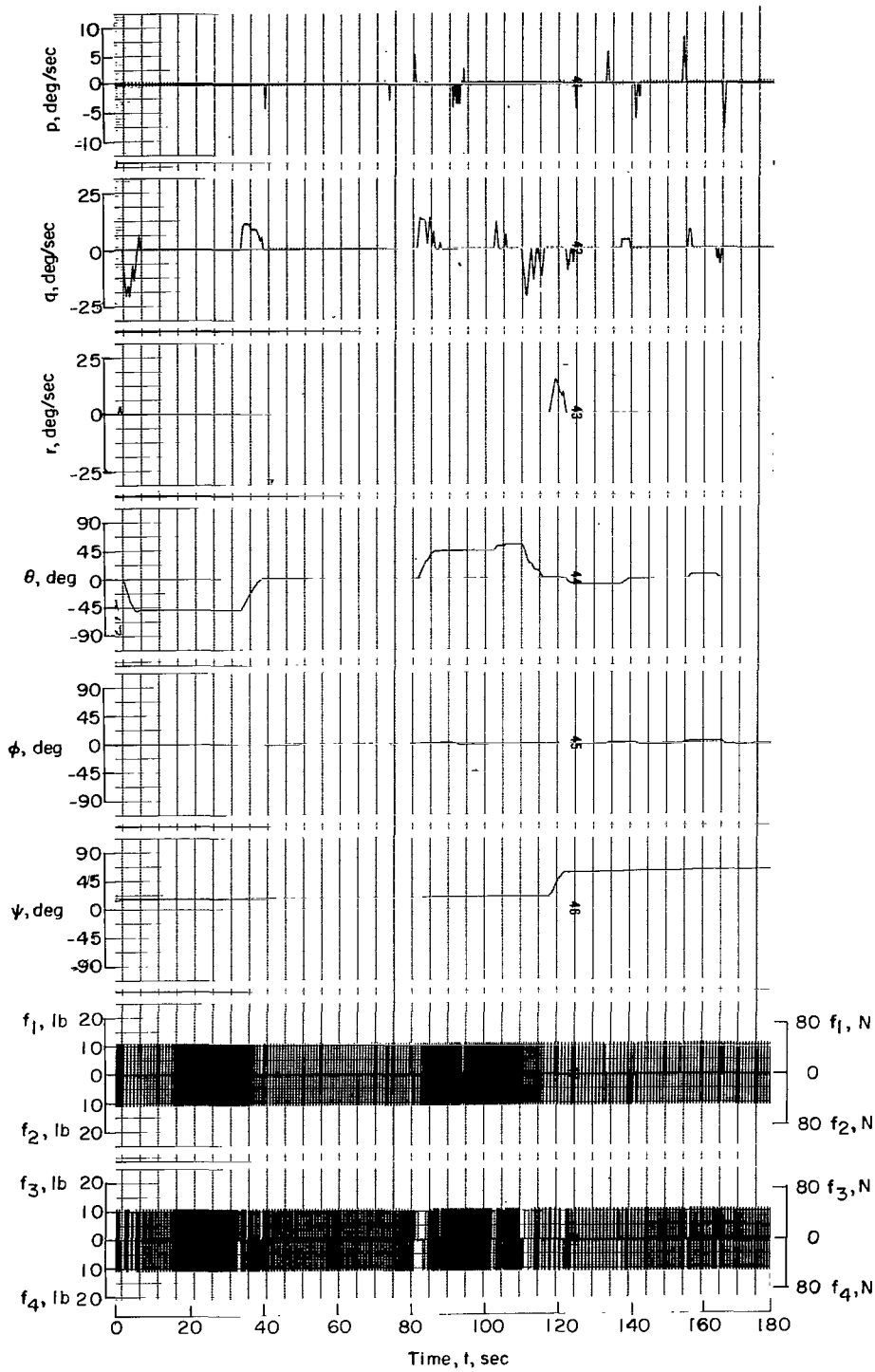

Figure 9.- Concluded.

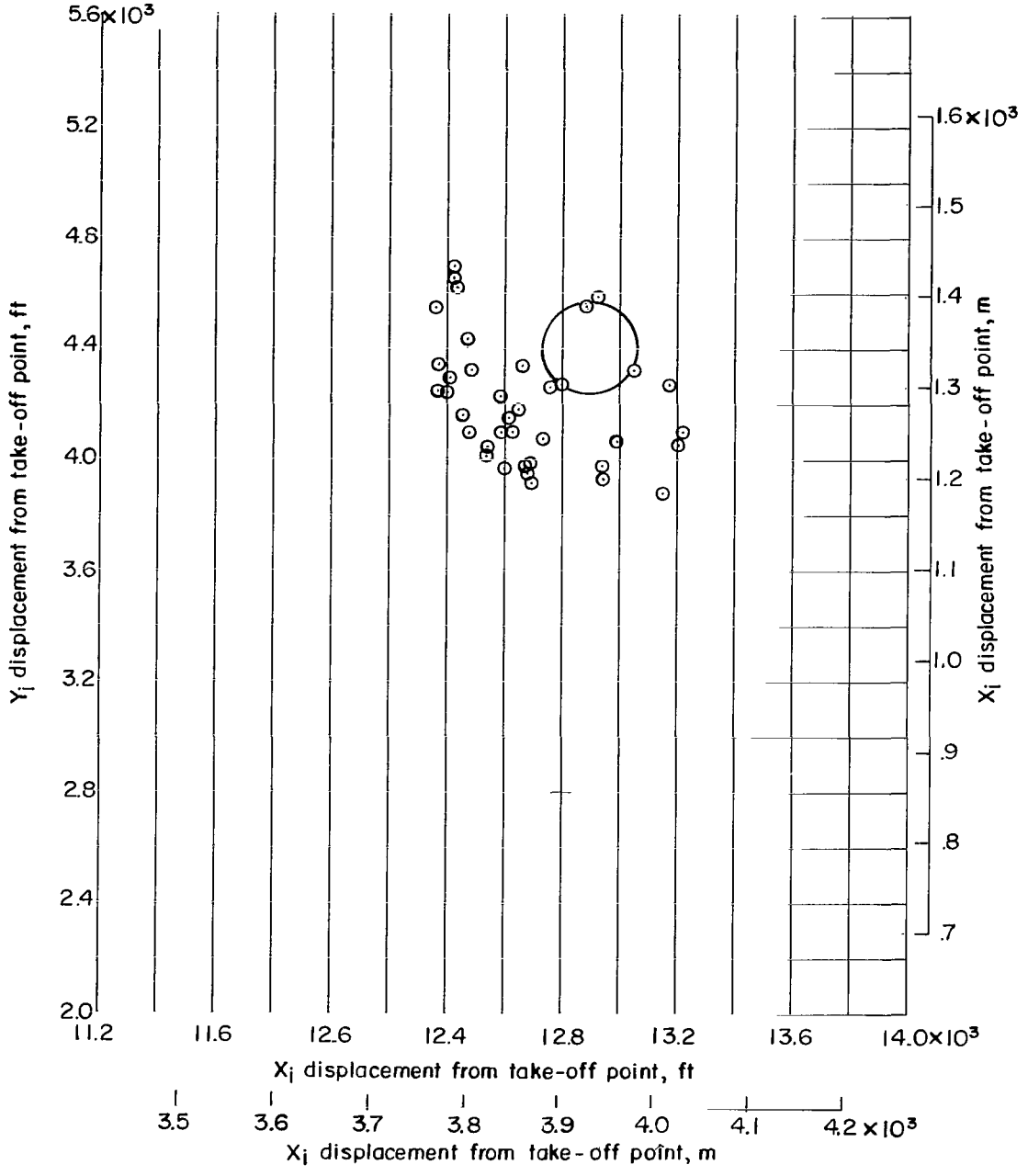

Figure 10.- Location of landing sites relative to target crater for flights using an altimeter and vertical- and horizontal-velocity indicators.

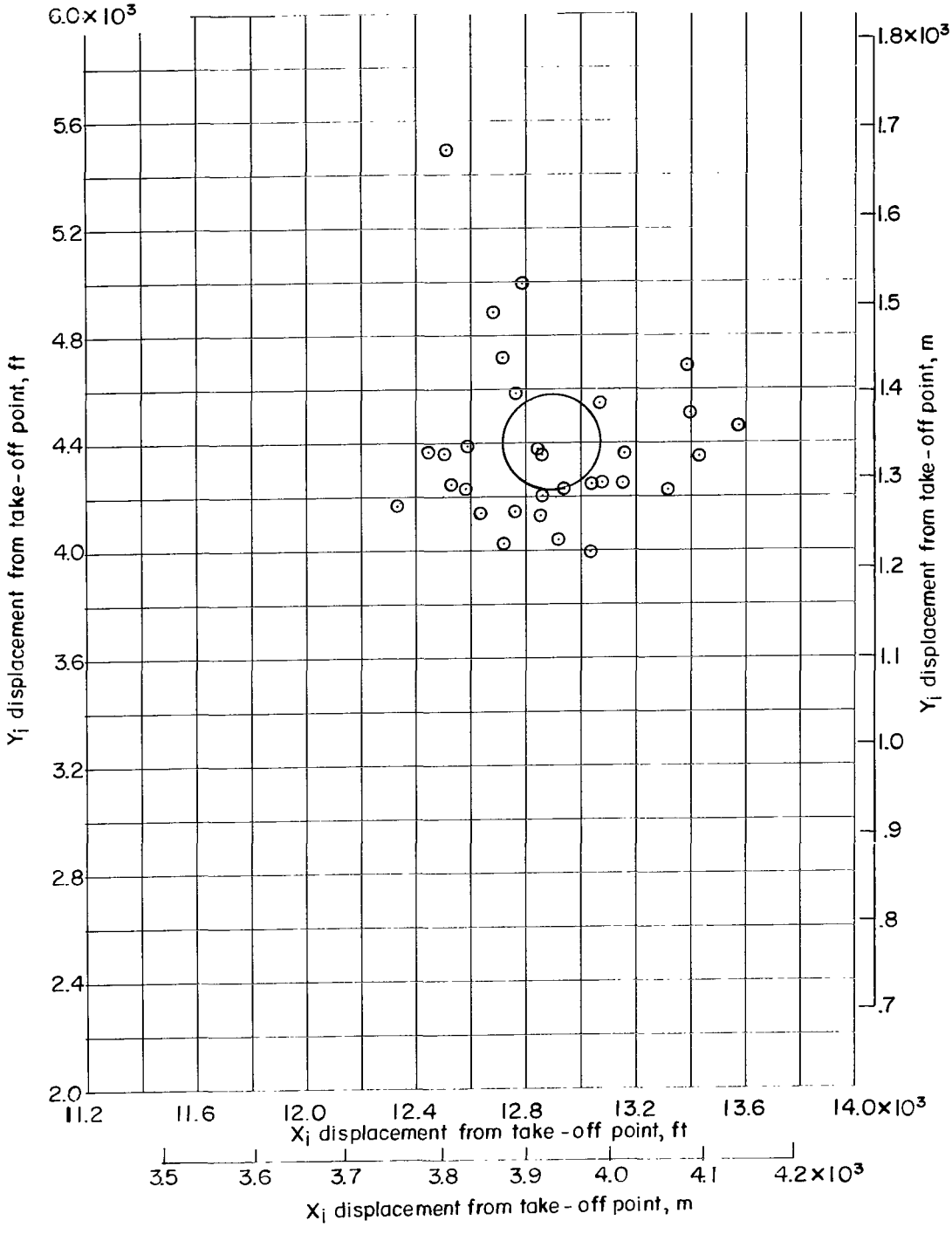

Figure 11.- Location of landing sites relative to target crater for flights performed without velocity or altitude indicators.

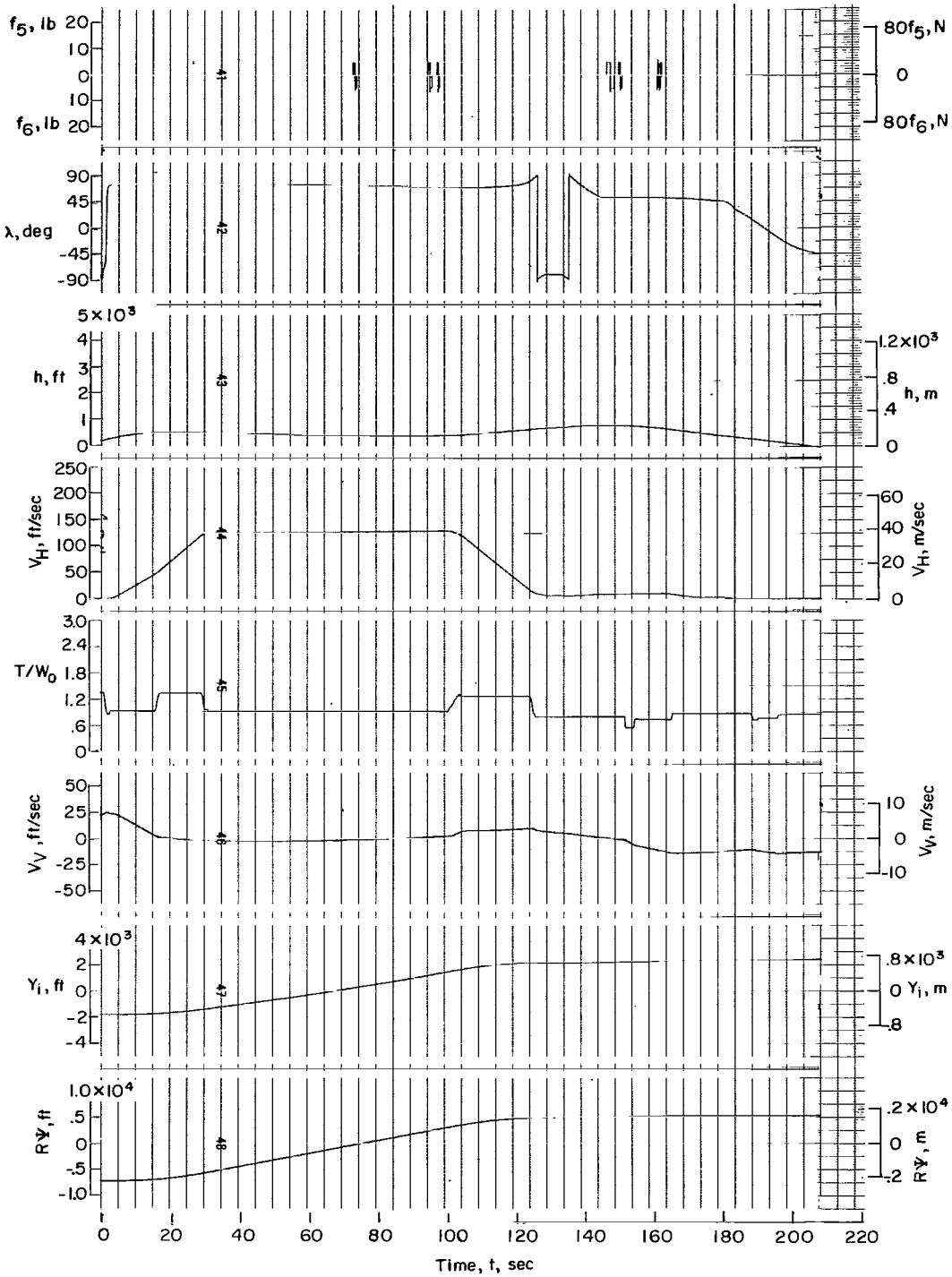

Figure 12.- Results of a typical flight performed without altitude or velocity indicators. (The rate deadband was 0.2°/sec.)

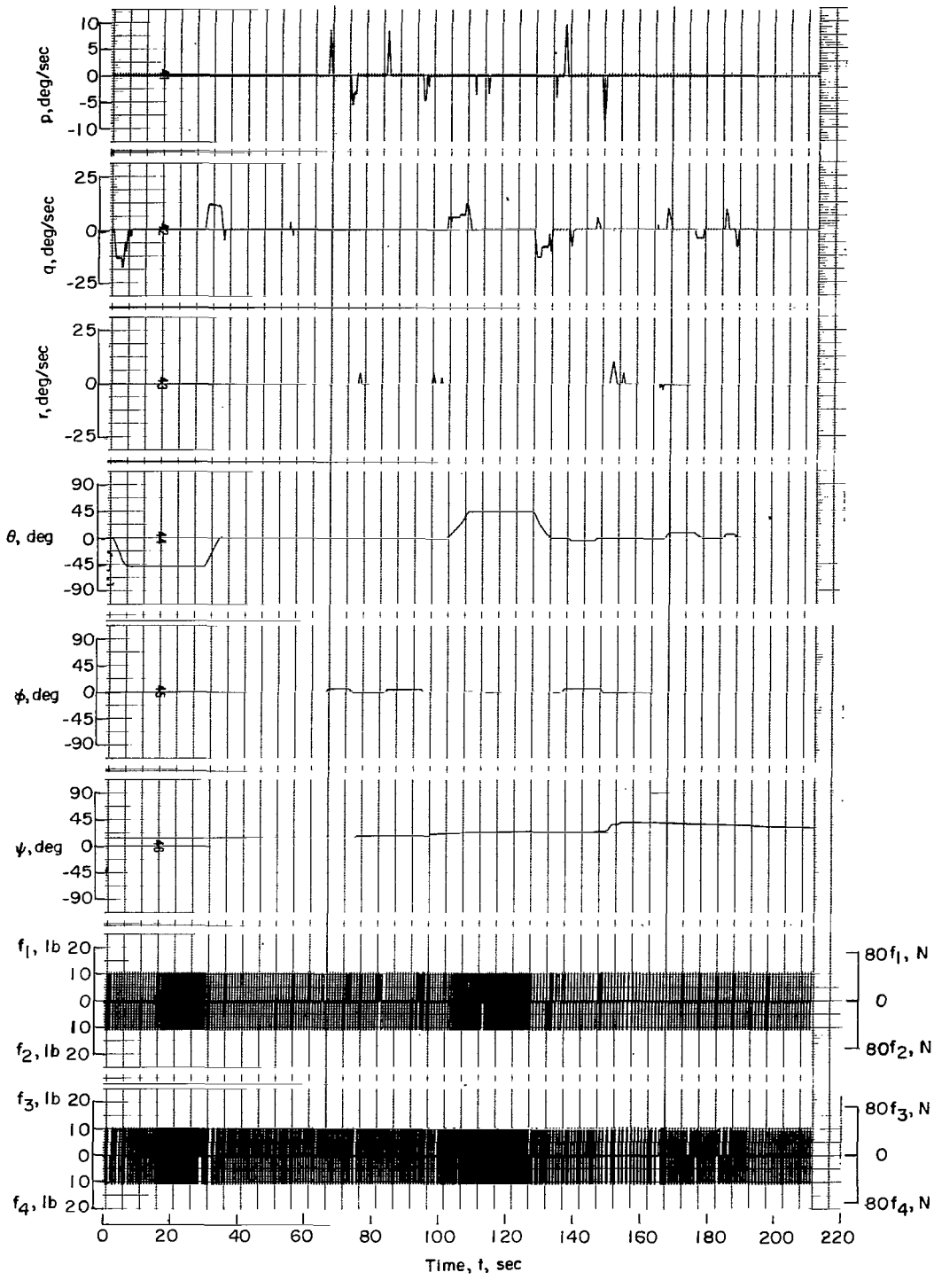

Figure 12.- Concluded.

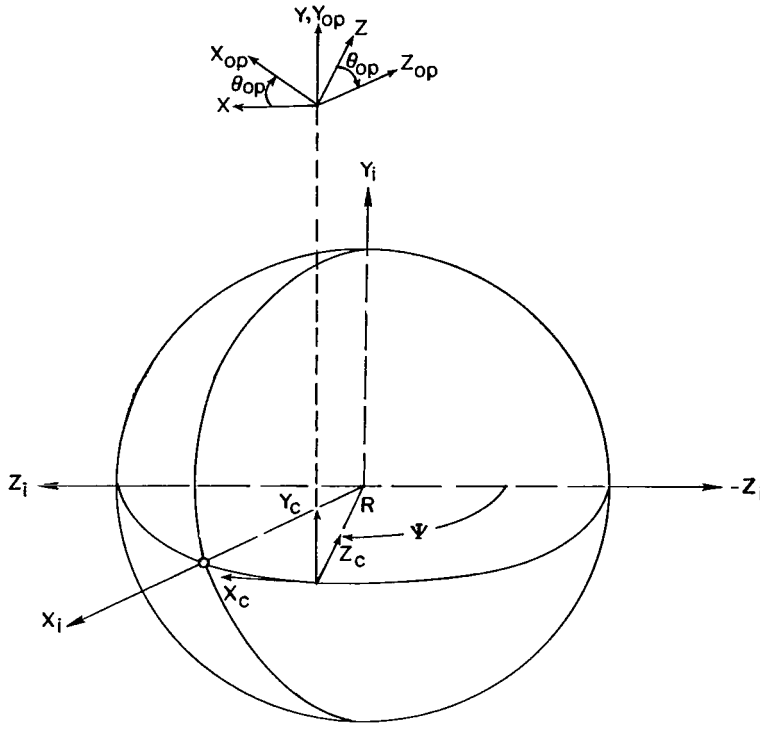

Figure 13.- Assumed axis systems.

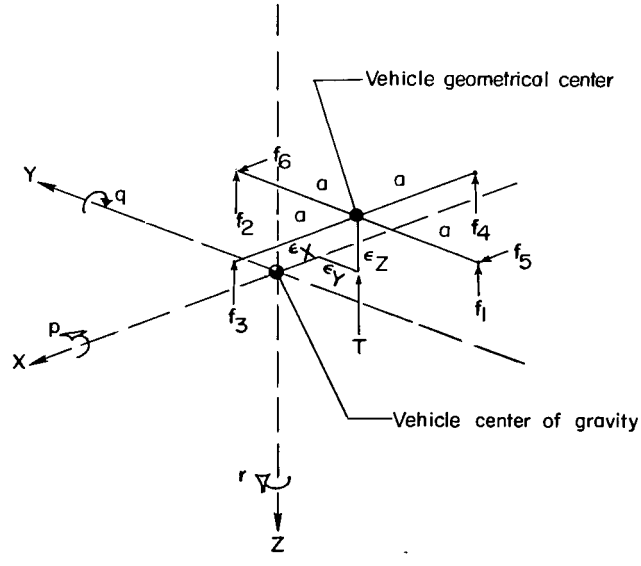

Figure 14.- Relation between body axes and vehicle geometry.

"The aeronautical and space activities of the United States shall be conducted so as to contribute . . . to the expansion of human knowledge of phenomena in the atmosphere and space. The Administration shall provide for the widest practicable and appropriate dissemination of information concerning its activities and the results thereof."

—NATIONAL AERONAUTICS AND SPACE ACT OF 1958

NASA SCIENTIFIC AND TECHNICAL PUBLICATIONS

TECHNICAL REPORTS: Scientific and technical information considered important, complete, and a lasting contribution to existing knowledge.

TECHNICAL NOTES: Information less broad in scope but nevertheless of importance as a contribution to existing knowledge.

TECHNICAL MEMORANDUMS: Information receiving limited distribution because of preliminary data, security classification, or other reasons.

CONTRACTOR REPORTS: Scientific and technical information generated under a NASA contract or grant and considered an important contribution to existing knowledge.

TECHNICAL TRANSLATIONS: Information published in a foreign language considered to merit NASA distribution in English.

SPECIAL PUBLICATIONS: Information derived from or of value to NASA activities. Publications include conference proceedings, monographs, data compilations, handbooks, sourcebooks, and special bibliographies.

TECHNOLOGY UTILIZATION PUBLICATIONS: Information on technology used by NASA that may be of particular interest in commercial and other non-aerospace applications. Publications include Tech Briefs, Technology Utilization Reports and Notes, and Technology Surveys.

Details on the availability of these publications may be obtained from:

SCIENTIFIC AND TECHNICAL INFORMATION DIVISION

NATIONAL AERONAUTICS AND SPACE ADMINISTRATION

Washington, D.C. 20546